EURASIP Journal on Wireless Communications and Networking
a SpringerOpen Journal

RESEARCH Open Access

Adaptive constrained CM-based multicarrier-CDMA receivers in multipath fading channels

Jun-Da Chen[1*] and Ye-Shun Shen[2]

Abstract

Two blind adaptive receivers, based on constrained constant modulus (CM) algorithms, are investigated for the detection of the multicarrier code division multiple access (MC-CDMA) system in the multiuser and multipath channels. As the data rate of the information bit is getting high enough, the transmitted signal of the MC-CDMA system becomes more sensitive to the frequency-selective fading. To mitigate this drawback, the parallel transmissions of multiple data symbols within one OFDM block are employed in the proposed systems to ensure that the length of the cyclic prefix (CP) is longer than the delay spread of the multipath channel. The first receiver is called a full-tap receiver (TDes receiver), which can carry out the interference suppression in the frequency-domain. Alternatively, a reduced-tap receiver (TRTap) is proposed on the basis of the derived cyclically shifting matrix. According to the derived matrix representation of the received signal, the analytical steady-state mean square errors (MSEs) for both receivers are also derived and compared. Simulation results are provided to illustrate the effectiveness of the proposed receivers and validate the accuracy of the theoretical analysis. As expected, the symbol error rate (SER) performance of the full-tap receiver is better than that of the reduced-tap receiver in severe interference environments. In contrast, the reduced-tap receiver can provide the satisfied SER performance just like the full-tap receiver in low-interference scenarios, even though the former one adopts only one-tap equalization.

Keywords: Multicarrier modulation; CDMA; Constant modulus; Adaptive filter

1 Introduction

Multicarrier (MC) modulation techniques have received great interest recently, because each data symbol is spread over several subcarriers in this scheme to obtain the frequency diversity of the transmission channel. Multicarrier code division multiple access (MC-CDMA) systems, which combine the direct-sequence code division multiple access (DS-CDMA) and the orthogonal frequency division multiplexing (OFDM) signal formats, can provide excellent system performance and flexibility to accommodate multimedia traffic. Instead of applying the spreading code to the time domain representation of the transmitted signal, such as the DS-CDMA system, MC-CDMA system maps some chips of a spreading sequence to several individual OFDM subcarriers [1,2]. Hence, the data rate of each OFDM subcarrier is identical to that of the input data. A cyclic prefix (CP), which is generally selected to be longer than the delay spread of the multipath channel, is inserted in the transmitted signal of the MC-CDMA system to maintain mutual orthogonality and independence among the subcarriers. Accordingly, the effect of the intersymbol interference (ISI) in MC-CDMA systems can be eliminated due to the CP insertion. However, similar to DS-CDMA systems, the performances of MC-CDMAs system are restricted by interferences, including the multiple access interference (MAI) and the intercarrier interference (ICI).

The blind adaptive equalization techniques, which can be applied to the aforementioned systems to resolve the interference problems and recover the transmission data, have received considerable attention. The most important advantage of the blind detection is to release the

*Correspondence: chenda888@just.edu.tw
[1] Institute of Computer and Communication Engineering, Jinwen University of Science and Technology, Taipei 231-54, Taiwan
Full list of author information is available at the end of the article

requirement of sending the training sequence and offer the higher data throughput. Some familiar blind multiuser detections, such as the minimum output energy (MOE) [3], the subspace approach [4], and the constant modulus approach (CMA) [5-10], have been investigated during the past decade. In [11], the constant modulus (CM)-based receivers were demonstrated that can perform almost as well as the non-blind/trained receivers if the undesirable local minima can be avoided. Consequently, the constrained version of CMA was designed to exclude the undesired local minima. Accordingly, a linearly constrained constant modulus (LCCM) receiver was proposed and analyzed in [5,6]. Specifically, by applying this constraint, the saddle stationary points do not exist in the convergence behavior of LCCM. Besides, the LCCM approach can completely remove MAI if the amplitude of the desired user is not less than the critical value in the noise-free environment. Therefore, the LCCM receiver is a good candidate in respect to the blind reception of the MC-CDMA system.

The blind adaptive equalizations of multiuser CDMA systems have been examined in many literatures, e.g., in [3-10,12-14]. However, the blind detections of MC-CDMA systems were discussed merely in a few papers, e.g., [15-23]. The subspace methods introduced in [15] and [16] were used to combat the impact of channel impairments. In addition, the zero forcing and decorrelating receivers for the multicarrier systems were also proposed in [17] and [18], respectively. In [19] and [20], the blind adaptive algorithms were adopted to recover the message symbols from the damaged signals. An important topic for the blind adaptive filter is its convergence behavior. The constrained MOE receivers mentioned in [21] and [22] can ensure that the filter's weight is able to converge to the desired user. At the transmitters of the MC-CDMA systems in [15-21], it is worthy to note that only one data symbol is spread in terms of a given spreading code within an OFDM symbol block. However, the transmitted signal becomes more sensitive to the frequency-selective fading as the transmission rate of the input data is getting high enough. To mitigate this problem, the input data should be first performed in a serial-to-parallel (S/P) conversion to extend the duration of the OFDM block before carrying out the spreading process in the frequency domain. In other words, multiple data symbols are simultaneously transmitted in one OFDM block (i.e., multiple symbols transmission). A constrained MOE-based minimum mean square error (MMSE) receiver was designed in [22] to realize the multiple symbols transmission. However, the number of the filter's tap used in the receiver has to be equal to the length of spreading code. In a low-interference scenario, a reduced-tap receiver can be employed to reduce the system complexity at the cost of the system performance. The reduced-tap equalizations have been examined in many literatures, e.g., [24-29]. However, the reduced-tap receivers for MC-CDMA systems were only discussed in a few papers. To reduce the complexity of DS-CDMA system, the received signal is passed through a bank of filters, called a cyclically shifted filter bank (CSFB), and each of which is a cyclically shifted version of the matched filter [30]. A decision statistic of the system is a linear combination of the output samples of the CSFB filters in a symbol interval. Because the dimension of the CSFB is generally smaller than the length of the spreading code, the CSFB detection can be implemented much more easily compared with the conventional MMSE detection. In this paper, we apply the CSFB scheme to construct the proposed reduced-tap MC-CDMA receivers. The reduction of the complexity of MC-CDMA system can be accomplished when the dimension of the signal subspace is smaller than that of the original filter used.

Two constrained CM-based algorithms, which can reduce the effects of MAI and ICI in MC-CDMA systems, are proposed in this paper. A constrained despreader (called TDes) receiver, which performs as the despreading process, is introduced in the next section. To provide the multiple symbols transmission, the proposed TDes receiver is designed as an extension of the LCCM scheme in [23] with which only one data symbol was considered and transmitted within an OFDM symbol duration. As the guard interval of an OFDM block is selected to be longer than the delay spread of the multipath fading, we can signify the effect of the multipath fading channel and the transform between the time-frequency domains in terms of multiplication of the matrices. According to this matrix representation, the performance of TDes receiver is theoretically derived and analyzed. However, the weight length (tap number) of TDes has to be the same as the length of the spreading code. With the matrix expression, we then formulate a CSFB matrix to construct a constrained reduced-tap (TRTap) receiver whose weight length can be far shorter than the length of the spreading code. For TRTap receiver, a multiplication of the lth row of the CSFB matrix and the vector denoted as the received signal is utilized to represent the demultipath and despreading processes for the lth multipath signal. If the tap's number of TRTap is large enough, a linear combination of the multiple multiplication results of the CSFB matrix and the received vector can be carried out to acquire the estimate of the data symbol. According to the Fourier transform matrix and CSFB matrix, we also derive the theoretical steady-state mean square errors (MSEs) of both TDes and TRTap schemes. We further illustrate the results of the steady-state MSEs in two special scenarios and conclude the following: (1) In cases of the multiusers' environment accompanied by a set of orthogonal spreading codes and in the absence of multipath fading, the selection of the

tap's number of TRTap has no great influence on the system performance, and the steady-state MSE of TRTap is nearly the same as that of TDes. (2) In cases of a single active user in presence of multipath fading, the performance of the steady-state MSE of TRTap with the tap's number close to the length of the spreading code can approach to that of TDes. As expected, TRTap, whose tap's number is equal to the spreading code's length, can provide better steady-state MSE performance than TRTap with a single tap.

This paper is organized as follows. In Section 2, the MC-CDMA multiuser communication system over multipath fading channel is introduced and modeled. Afterward, two constrained CM-based MC-CDMA receivers are proposed in Section 3. In Section 4, the steady-state MSE performances of the proposed schemes are theoretically analyzed and compared. In Section 5, simulation results are given to demonstrate the effectiveness of the proposed receivers. Finally, the conclusions are drawn in the last section.

2 System description

The baseband structure of MC-CDMA transmitter in the downlink MC-CDMA system under multipath fading channels is shown in Figure 1. Assume that there are totally K active users accessing this multicarrier system simultaneously, and each of them transmits ς data symbols in parallel within each data block. In the nth data block (OFDM symbol) with duration T_b, totally ς data symbols (i.e., ς phase-shift keying (PSK) or quadrature amplitude modulation (QAM) data symbols) of the kth user are encapsulated into one data block and denoted by $\mathbf{d}^{(k)}(n) = \left[d_0^{(k)}(n), d_1^{(k)}(n), \ldots, d_{\varsigma-1}^{(k)}(n)\right]$, $k \in \{0, 1, \ldots, K-1\}$. Afterward, each data block of the kth user, $\mathbf{d}^{(k)}(n)$, is the first serial-to-parallel (S/P) converted and transmitted in parallel in order to extend the symbol duration of PSK modulation in the proposed MC-CDMA system. Subsequently, each of the ς data symbols is spread over the frequency domain in terms of the specific spreading code of kth user, $\mathbf{c}^{(k)} = \left[c_0^{(k)}, c_1^{(k)}, \ldots, c_{G-1}^{(k)}\right]^{\mathrm{T}}$, where $c_l^{(k)}$ is the lth chip of the spreading code. The sequence of the nth data block can be expressed as

$$\left[d_0^{(k)}c_0^{(k)}, \ldots, d_0^{(k)}c_{G-1}^{(k)}, \ldots, d_{\varsigma-1}^{(k)}c_0^{(k)}, \ldots, d_{\varsigma-1}^{(k)}c_{G-1}^{(k)}\right]^{\mathrm{T}} \tag{1}$$

where G is the processing gain and $[\bullet]^{\mathrm{T}}$ denotes the transposition operation. The sequence of each data block has to be interleaved such that G consecutive chips in (1) (corresponds to a single PSK symbol) can be approximately transmitted over G-independent fading subchannels. As the simple frequency interleaving and deinterleaving methods are applied in the proposed system, the similar symbol error rate (SER) for the detection of PSK-modulated symbol in [31] can be achieved. After carrying out interleaving process, the sequence of a data block becomes

$$\mathbf{s}^{(k)} = \left[d_0^{(k)}c_0^{(k)}, \ldots, d_{\varsigma-1}^{(k)}c_0^{(k)}, \ldots, d_0^{(k)}c_{G-1}^{(k)}, \ldots, d_{\varsigma-1}^{(k)}c_{G-1}^{(k)}\right]^{\mathrm{T}}. \tag{2}$$

Totally, $N_c(=\varsigma G)$ chips in (2) are transmitted over N_c orthogonal subcarriers with the frequency separation of $\Delta f = 1/T_b$ based on the OFDM modulation, which can be easily implemented by applying the inverse fast Fourier transform (IFFT) to the frequency interleaver's outputs. Consequently, the time-domain transmitted signal of the kth user can be expressed as $\mathbf{t}^{(k)} = \mathbf{F}^{\mathrm{H}}\mathbf{s}^{(k)}$, where $\mathbf{F}$ and $[\bullet]^{\mathrm{H}}$ denote the $N_c \times N_c$ Fourier matrix and Hermitian

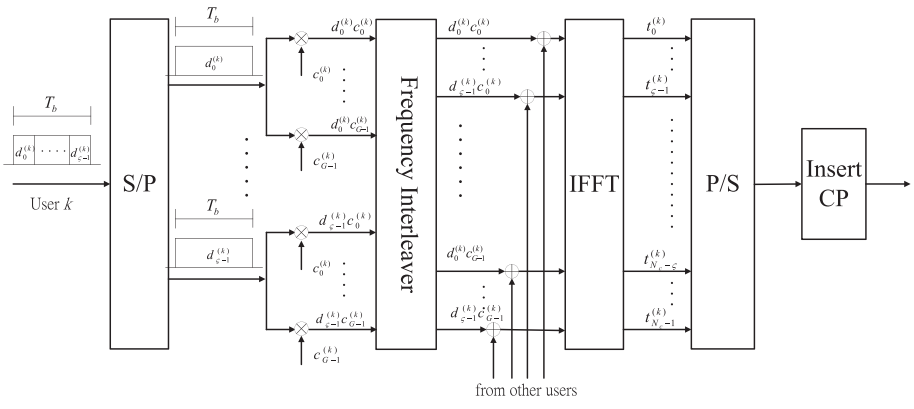

Figure 1 The block diagram of a MC-CDMA transmitter.

transposition, respectively. The rth element (time sample) of the kth user's transmitted signal is denoted as

$$t_r^{(k)} = \frac{1}{\sqrt{N_c}} \sum_{p=0}^{G-1} c_p^{(k)} \sum_{m=0}^{\varsigma-1} d_m^{(k)} (w^{(m+p\varsigma)\times r})^* \tag{3}$$

where $w = e^{-j2\pi/N_c}$ and $(\bullet)^*$ is the complex conjugate operation. After rearranging for the summation's order in (3), we can rewrite $t_r^{(k)}$ as follows:

$$t_r^{(k)} = \frac{1}{\sqrt{N_c}} \sum_{m=0}^{\varsigma-1} d_m^{(k)} \sum_{p=0}^{G-1} c_p^{(k)} (w^{(m+p\varsigma)\times r})^*. \tag{4}$$

Subsequently, we can further express the transmitted signal of the kth user, $\mathbf{t}^{(k)}(n)$, in terms of ς PSK symbols $d_m^{(k)}$. We define a $G \times N_c$-modified Fourier matrix $\mathbf{F}_m$ whose rows are extracted from the rows of Fourier matrix $\mathbf{F}$ with ς separations, where $m \in \{0, 1, \ldots, \varsigma - 1\}$. Therefore, the pth row of $\mathbf{F}_m$ is

$$\mathbf{f}_m^{(p)} = \frac{1}{\sqrt{N_c}} \left[w^{(p\varsigma+m)\times 0}, w^{(p\varsigma+m)\times 1} \ldots, w^{(p\varsigma+m)\times(N_c-1)} \right]. \tag{5}$$

It is worthy to mention that the properties of $\mathbf{F}_m$, $\mathbf{F}_m\mathbf{F}_m^{\mathrm{H}} = \mathbf{I}$ and $\mathbf{F}_m^{\mathrm{H}}\mathbf{F}_m \neq \mathbf{I}$, can be derived and shown in Appendix 1, where $\mathbf{I}$ is the identity matrix. Before the insertion of the CP, the time-domain transmitted signal for all K users in the nth (OFDM) symbol duration is written as

$$\mathbf{t}(n) = \sum_{k=0}^{K-1} \mathbf{t}^{(k)}(n) = \sum_{k=0}^{K-1} \sum_{m=0}^{\varsigma-1} d_m^{(k)}(n) \mathbf{F}_m^{\mathrm{H}} \mathbf{c}^{(k)} \tag{6}$$

where $\mathbf{t}^{(k)}(n) = \left[t_0^{(k)}, t_1^{(k)}, \ldots, t_{N_c-1}^{(k)} \right]^{\mathrm{T}}$ is the time domain signal transmitted for the kth user. After the parallel-to-serial (P/S) conversion for $\mathbf{t}(n)$ in (6), CP is then added to eliminate the interference between consecutive OFDM symbols.

A discrete impulse response of the multipath fading channel with N_P paths is modeled as $h(t) = \sum_{l=0}^{N_P-1} h_l \delta(t - \tau_l)$, where h_l and τ_l denote the path gain and the path delay of the lth path, respectively. If the CP is longer than the multipath spread and the synchronization of the received signal is perfect, there is no ISI between any two successive OFDM blocks. Thus, we just need to concentrate on one OFDM block after removing the CP. To express the received signal, the usage of CP results to a circular convolution between the transmitted signal and the channel impulse response [32]. Define $\mathbf{t}(n; l)$ as the lth delayed path of the received signal. The delayed path is equivalent to the cyclic shift of the direct (first) path because the guard interval in the form of CP is appended in front of each OFDM block. Define $\mathbf{I}_l$ as a shifting matrix which circularly shifts each column of the identity matrix $\mathbf{I}$ down by l rows. Hence, the (r, s)th element of $\mathbf{I}_l$ is

$$i_{r,s} = \begin{cases} 1; & \text{if } r - s = l \text{ or } r + N_c - s = l \\ 0; & \text{others.} \end{cases} \tag{7}$$

Note that $\mathbf{I}_0 = \mathbf{I}$. In terms of the shifting matrix $\mathbf{I}_l$, the lth delayed path can be expressed with relation to the direct path, that is, $\mathbf{t}(n; l) = \mathbf{I}_l \mathbf{t}(n)$.

The blind synchronization algorithms for jointly estimating timing and frequency offset in multicarrier systems have been proposed in some literatures [33-36]. The perfect synchronization is assumed and the synchronization issue is not discussed in this paper. After accomplishing the perfect synchronization and removing CP, the received signal in the time domain thus can be modeled as

$$\begin{aligned} \mathbf{r}(n) &= \sum_{l=0}^{N_P-1} h_l \mathbf{t}(n; l) + \mathbf{g}(n) \\ &= \sum_{l=0}^{N_P-1} h_l \mathbf{I}_l \sum_{k=0}^{K-1} \sum_{m=0}^{\varsigma-1} d_m^{(k)}(n) \mathbf{F}_m^{\mathrm{H}} \mathbf{c}^{(k)} + \mathbf{g}(n) \\ &= \mathbf{H} \sum_{m=0}^{\varsigma-1} \mathbf{F}_m^{\mathrm{H}} \mathbf{C} \mathbf{d}_m(n) + \mathbf{g}(n) \end{aligned} \tag{8}$$

where $\mathbf{g}(n)$ is the additive white Gaussian noise (AWGN) vector and the channel matrix $\mathbf{H} = \sum_{l=0}^{N_P-1} h_l \mathbf{I}_l$ acts as the channel effect of the multipath fading on the received signal. The code matrix $\mathbf{C}$ is composed of the spreading codes of all active users, where the kth column of $\mathbf{C}$ is equal to $\mathbf{c}^{(k)}$. The data vector $\mathbf{d}_m(n)$ is composed of the mth PSK symbol of all active users within nth OFDM symbol block, where the kth element of $\mathbf{d}_m(n)$ is $d_m^{(k)}(n)$.

At the receiver of the desired user, after removing the CP, a square FFT matrix of size N_c, $\mathbf{F}$, is performed to convert the received signal from time domain to frequency domain, i.e., $\widetilde{\mathbf{r}}(n) = \mathbf{F}\mathbf{r}(n) = [\widetilde{r}_0(n), \widetilde{r}_1(n), \ldots, \widetilde{r}_{N_c-1}(n)]^{\mathrm{T}}$, and then frequency deinterleaving carries out. Because $\mathbf{F}\mathbf{I}_l\mathbf{F}^{\mathrm{H}}$ is a diagonal matrix (similar derivation will be shown later), the rows of $\mathbf{F}\mathbf{I}_l\mathbf{F}_m^{\mathrm{H}}$ become zero vector besides the rows $r\varsigma + m$, where $r \in \{0, 1, \ldots, G-1\}$. We only need to consider all of the non-zero rows of $\widetilde{\mathbf{r}}(n)$ if the specific PSK data symbol $d_m^{(k)}(n)$ is to be estimated. Accordingly, $\widetilde{\mathbf{r}}_m(n)$ is defined as a $G \times 1$ post-FFT vector whose elements are extracted from those of $\widetilde{\mathbf{r}}(n)$ with ς separations, i.e., $\widetilde{\mathbf{r}}_m(n) = \left[\widetilde{r}_{0\times\varsigma+m}(n), \widetilde{r}_{1\times\varsigma+m}(n), \ldots, \widetilde{r}_{(G-1)\times\varsigma+m}(n)\right]^{\mathrm{T}}$. After ignoring the all-zero rows, we can express all of the

non-zero rows of $\mathbf{F}\mathbf{I}_l\mathbf{F}_m^{\mathrm{H}}$ as $\mathbf{F}_m\mathbf{I}_l\mathbf{F}_m^{\mathrm{H}}$. Thus, the received signal before despreading process is expressed as

$$\widetilde{\mathbf{r}}_m(n) = \mathbf{F}_m\mathbf{H}\mathbf{F}_m^{\mathrm{H}}\mathbf{C}\mathbf{d}_m(n) + \mathbf{F}_m\mathbf{g}(n). \tag{9}$$

Due to no ISI, the time index n can be ignored, i.e., $d_m^{(k)}(n)$ becomes $d_m^{(k)}$, besides filter's weight in the following derivation. For convenience, let the first user be the desired user.

3 Constrained CM-based MC-CDMA receiver

To design the MC-CDMA receiver structure, our goal is to determine a FIR filter that provides an estimation of the desired symbol by the hard-decision result of the filter output under the particular constraint. For the constrained optimization problems, several adaptive methods can be chosen as shown in [12]. The complexity of recursive least squares (RLS) algorithm is more complicated because of the computation of the inverse of the correlation matrix of the input vector. Thus, in this paper, the generalized sidelobe canceler (GSC) structure is used, which can be thought as an updating rule of the equivalent problem without constraints. In the following, two adaptive constrained CM-based receivers called TDes and TRTap are proposed and examined. For the constant modulus algorithm, the cost function is modeled as

$$E\left[(|y|^2 - \nu)^2\right]$$

where y is the filter's output and ν is the variance of the desired modulation signal or $E\{|d_m^{(k)}|^4\}/E\{|d_m^{(k)}|^2\}$.

3.1 Constrained despreader

For the estimation of mth PSK symbol within nth OFDM symbol block, the filter's coefficients, $\mathbf{w}(n)$, in the TDes are designed according to the following minimization problem

$$\min J(\mathbf{w}) = E\left[(|y|^2 - \nu)^2\right] \text{ subject to } \mathbf{w}^{\mathrm{H}}(n)\mathbf{F}_m\mathbf{H}\mathbf{F}_m^{\mathrm{H}}\mathbf{c}^{(0)} = 1 \tag{10}$$

where $E[\bullet]$ means that the expectation operation and y is obtained as $\mathbf{w}^{\mathrm{H}}(n)\widetilde{\mathbf{r}}_m$. Based on the constraint, $\mathbf{w}^{\mathrm{H}}(n)\mathbf{F}_m\mathbf{H}\mathbf{F}_m^{\mathrm{H}}\mathbf{c}^{(0)} = 1$, the filter's output is ensured to converge to the data symbol of desired user, $d_m^{(0)}$, which can be easily proven by the similar procedure as in [5,6]. Afterward, the recursive equation of the filter's weight for the proposed receiver is derived. The similar derivation for blind DS-CDMA receiver can be referred in [12,13]. From (10), the Lagrangian cost function can be shown as follows:

$$L = |\mathbf{w}^{\mathrm{H}}(n)\widetilde{\mathbf{r}}_m\widetilde{\mathbf{r}}_m^{\mathrm{H}}\mathbf{w}(n) - \nu|^2 - \lambda^*(\mathbf{w}^{\mathrm{H}}(n)\mathbf{F}_m\mathbf{H}\mathbf{F}_m^{\mathrm{H}}\mathbf{c}^{(0)} - 1)$$

where λ is the Lagrangian multiplier. Define $\varphi = \widetilde{\mathbf{r}}_m\widetilde{\mathbf{r}}_m^{\mathrm{H}}$, $\varepsilon = \mathbf{w}^{\mathrm{H}}(n)\varphi\mathbf{w}(n) - \nu$, and $\mathbf{F}_m\mathbf{H}\mathbf{F}_m^{\mathrm{H}} = \widetilde{\mathbf{F}}_m$. Then, the gradient of the cost function with respect to $\mathbf{w}(n)$ becomes

$$\frac{\partial L}{\partial \mathbf{w}(n)} = \varepsilon\varphi\mathbf{w}(n) - \lambda^*\widetilde{\mathbf{F}}_m\mathbf{c}^{(0)}. \tag{11}$$

By steepest-descent method, the recursive equation of the filter's weight is written as

$$\mathbf{w}(n+1) = \mathbf{w}(n) - \frac{1}{2}\mu\{\varepsilon\varphi\mathbf{w}(n) - \lambda^*\widetilde{\mathbf{F}}_m\mathbf{c}^{(0)}\} \tag{12}$$

where μ is step size. It is worthy to note that the filter's weight also satisfies the constraint $(\mathbf{c}^{(0)})^{\mathrm{H}}\widetilde{\mathbf{F}}_m^{\mathrm{H}}\mathbf{w}(n+1) = 1$. Thus, by substituting (12) into the previous constraint and rearranging it, the Lagrangian multiplier can be written as

$$\lambda^* = -(\frac{2}{\mu\alpha})(\mathbf{c}^{(0)})^{\mathrm{H}}\widetilde{\mathbf{F}}_m^{\mathrm{H}}\mathbf{w}(n) + \frac{\varepsilon}{\alpha}(\mathbf{c}^{(0)})^{\mathrm{H}}\widetilde{\mathbf{F}}_m^{\mathrm{H}}\varphi\mathbf{w}(n) + (\frac{2}{\mu\alpha}) \tag{13}$$

where $\alpha = (\mathbf{c}^{(0)})^{\mathrm{H}}\widetilde{\mathbf{F}}_m^{\mathrm{H}}\widetilde{\mathbf{F}}_m\mathbf{c}^{(0)}$. Substituting (13) into (12) and letting $\widetilde{\mathbf{P}} = \frac{1}{\alpha}\widetilde{\mathbf{F}}_m\mathbf{c}^{(0)}(\mathbf{c}^{(0)})^{\mathrm{H}}\widetilde{\mathbf{F}}_m^{\mathrm{H}}$, we have

$$\mathbf{w}(n+1) = \mathbf{w}(n) - \frac{1}{2}\mu\varepsilon\{\mathbf{I} - \widetilde{\mathbf{P}}\}\varphi\mathbf{w}(n) - \widetilde{\mathbf{P}}\mathbf{w}(n) + \frac{1}{\alpha}\widetilde{\mathbf{F}}_m\mathbf{c}^{(0)} \tag{14}$$

The constrained optimization problem can be converted into an unconstrained form by using the GSC decomposition [5,13,37]

$$\mathbf{w}(n) = \mathbf{w}_q - \mathbf{B}\mathbf{w}_a(n)$$

where $\mathbf{w}_q$ is the constrained fixed portion of the weight vector, and $\mathbf{B}$ is a non-adaptive blocking matrix. The blocking matrix $\mathbf{B}$ must satisfy two conditions: $\mathbf{B}^{\mathrm{H}}\mathbf{B} = \mathbf{I}$ and $\mathbf{B}^{\mathrm{H}}\widetilde{\mathbf{F}}_m^{\mathrm{H}}\mathbf{c}^{(0)} = \mathbf{0}$. One method for constructing $\mathbf{B}$ is to find $\mathbf{P} = \mathbf{I} - \widetilde{\mathbf{P}}$. Then, we orthonormalize $\mathbf{P}$ and choose the columns of the orthonormalized matrix. To evaluate $\mathbf{w}_q$, we first need to find the optimal weight $\mathbf{w}_{\mathrm{o}}$ of the proposed TDes. From (11), by setting $\frac{\partial L}{\partial \mathbf{w}(n)} = 0$ and rearranging it, we have

$$\mathbf{w} = \frac{\lambda^*}{\varepsilon}\varphi^{-1}\widetilde{\mathbf{F}}_m\mathbf{c}^{(0)}. \tag{15}$$

Substituting (15) into the constraint $(\mathbf{c}^{(0)})^{\mathrm{H}}\widetilde{\mathbf{F}}_m^{\mathrm{H}}\mathbf{w} = 1$ and rearranging it, we have

$$\lambda^* = \varepsilon\left[(\mathbf{c}^{(0)})^{\mathrm{H}}\widetilde{\mathbf{F}}_m^{\mathrm{H}}\varphi^{-1}\widetilde{\mathbf{F}}_m\mathbf{c}^{(0)}\right]^{-1}.$$

Substituting the above equation into (15), the optimal weight $\mathbf{w}_{\mathrm{o}}$ can thus be written as

$$\mathbf{w}_{\mathrm{o}} = \varphi^{-1}\widetilde{\mathbf{F}}_m\mathbf{c}^{(0)}\left[(\mathbf{c}^{(0)})^{\mathrm{H}}\widetilde{\mathbf{F}}_m^{\mathrm{H}}\varphi^{-1}\widetilde{\mathbf{F}}_m\mathbf{c}^{(0)}\right]^{-1}. \tag{16}$$

In the GSC filter, $\mathbf{w}_q$ can be obtained as

$$\mathbf{w}_q = \widetilde{\mathbf{P}}\mathbf{w}_{\mathrm{o}} = \frac{1}{\alpha}\widetilde{\mathbf{F}}_m\mathbf{c}^{(0)}.$$

Applying $\mathbf{I} - \widetilde{\mathbf{P}} = \mathbf{P}$ and $\widetilde{\mathbf{F}}_m\mathbf{c}^{(0)}/\alpha = \mathbf{w}_q$ into (14), the updated equation can be rewritten as

$$\mathbf{w}(n+1) = \mathbf{P}\left[\mathbf{I} - \frac{1}{2}\mu\varepsilon\varphi\right]\mathbf{w}(n) + \mathbf{w}_q.$$

Substituting $\mathbf{w}(n+1) = \mathbf{w}_q - \mathbf{B}\mathbf{w}_a(n+1)$ into above equation and rearranging it, we obtain

$$\mathbf{B}\mathbf{w}_a(n+1) = \mathbf{P}\mathbf{B}\mathbf{w}_a(n) - \frac{1}{2}\mu\varepsilon\mathbf{P}\varphi\mathbf{B}\mathbf{w}_a(n) - \mathbf{P}\mathbf{w}_q + \frac{1}{2}\mu\varepsilon\mathbf{P}\varphi\mathbf{w}_q.$$

Multiplying $\mathbf{B}^{\mathrm{H}}$ on both sides of the above equation and utilizing the property of $\mathbf{B}$, the unconstrained adaptive weight vector $\mathbf{w}_a(n)$ thus can be updated as

$$\mathbf{w}_a(n+1) = \mathbf{w}_a(n) + \frac{1}{2}\mu\varepsilon\mathbf{B}^{\mathrm{H}}\varphi\left[\mathbf{w}_q - \mathbf{B}\mathbf{w}_a(n)\right].$$

The computation of TDes can be summarized as follows:

1. Compute $\alpha = (\mathbf{c}^{(0)})^{\mathrm{H}}\widetilde{\mathbf{F}}_m^{\mathrm{H}}\widetilde{\mathbf{F}}_m\mathbf{c}^{(0)}$
2. Compute $\mathbf{w}_q = \frac{1}{\alpha}\widetilde{\mathbf{F}}_m\mathbf{c}^{(0)}$
3. Orthonormalize $\mathbf{P} = \mathbf{I} - \frac{1}{\alpha}\widetilde{\mathbf{F}}_m\mathbf{c}^{(0)}(\mathbf{c}^{(0)})^{\mathrm{H}}\widetilde{\mathbf{F}}_m^{\mathrm{H}}$ and construct $\mathbf{B}$ from the orthonormalized matrix
4. Compute $\mathbf{w}(n) = \mathbf{w}_q - \mathbf{B}\mathbf{w}_a(n)$
5. Compute $y = \mathbf{w}^{\mathrm{H}}(n)\widetilde{\mathbf{r}}_m$
6. Compute $\varphi = \widetilde{\mathbf{r}}_m\widetilde{\mathbf{r}}_m^{\mathrm{H}}$, $\varepsilon = \mathbf{w}^{\mathrm{H}}(n)\varphi\mathbf{w}(n) - \nu$
7. Update the filter weight by $\mathbf{w}_a(n+1) = \mathbf{w}_a(n) + \frac{1}{2}\mu\varepsilon\mathbf{B}^{\mathrm{H}}\varphi\mathbf{w}(n)$

3.2 Constrained reduced-tap receiver

For TDes, the weight number of adaptive filter must equal to the code length. However, in a low MAI and ICI environment, a large number of filter weights is not necessary. For TRTap, the filter is designed by the functions of demultipath and despreading, and the length of filter weights is not restricted to the same length of the spreading code. First, we observe received signal before despreading $\widetilde{\mathbf{r}}_m(n)$. When ignoring the noise term, from (9), the received signal from path l can be expressed as $h_l\mathbf{F}_m\mathbf{I}_l\mathbf{F}_m^{\mathrm{H}}\mathbf{C}\mathbf{d}_m(n)$. Thus, the demultipath and despreading results of the received signal from path l can be written as

$$(\mathbf{c}^{(0)})^{\mathrm{H}}\mathbf{F}_m\mathbf{I}_l^{\mathrm{H}}\mathbf{F}_m^{\mathrm{H}}\mathbf{F}_m\mathbf{I}_l\mathbf{F}_m^{\mathrm{H}}\mathbf{C}\mathbf{d}_m(n). \tag{17}$$

It can be shown in Appendix 2 that

$$\mathbf{F}_m\mathbf{I}_l^{\mathrm{H}}\mathbf{F}_m^{\mathrm{H}}\mathbf{F}_m\mathbf{I}_l\mathbf{F}_m^{\mathrm{H}} = \mathbf{I}. \tag{18}$$

According to the property of (17), we set a $z\times G$ matrix

$$\mathbf{A} = \begin{bmatrix} (\mathbf{c}^{(0)})^{\mathrm{H}}\mathbf{F}_m\mathbf{I}_0^{\mathrm{H}}\mathbf{F}_m^{\mathrm{H}} \\ \vdots \\ (\mathbf{c}^{(0)})^{\mathrm{H}}\mathbf{F}_m\mathbf{I}_{z-1}^{\mathrm{H}}\mathbf{F}_m^{\mathrm{H}} \end{bmatrix} \tag{19}$$

where z is the tap length of TRTap and we set $z \le N_c/\varsigma$. Matrix $\mathbf{A}$ has the similar form as CSFB in [30]. Some properties of $\mathbf{A}$ are shown in Appendices 2 and 3. In Appendix 2, we show that $\mathbf{A}\mathbf{A}^{\mathrm{H}} = \mathbf{I}$ as $z \le N_c/\varsigma$ and $\mathbf{A}\mathbf{A}^{\mathrm{H}} \ne \mathbf{I}$ as $z > N_c/\varsigma$. In Appendix 3, we show that $\mathbf{A}^{\mathrm{H}}\mathbf{A} = \mathbf{I}$ when $z = N_c/\varsigma$. The filter output of TRTap thus can be written as

$$\widehat{y} = \widehat{\mathbf{w}}^{\mathrm{H}}\mathbf{A}\widetilde{\mathbf{r}}_m.$$

It is the linear combination of despreading result of each path. The constraint is set as $\widehat{\mathbf{w}}^{\mathrm{H}}(n)\mathbf{A}\mathbf{F}_m\mathbf{H}\mathbf{F}_m^{\mathrm{H}}\mathbf{c}^{(0)} = 1$ to ensure that the filter can converge to the information of desired user. The constrained cost function of TRTap thus can be written as

$$\min\widehat{J}(\widehat{\mathbf{w}}) = E\left[(|\widehat{\mathbf{w}}^{\mathrm{H}}\mathbf{A}\widetilde{\mathbf{r}}_m|^2 - \nu)^2\right] \text{ subject to } \widehat{\mathbf{w}}^{\mathrm{H}}(n) \times \mathbf{A}\mathbf{F}_m\mathbf{H}\mathbf{F}_m^{\mathrm{H}}(n)\mathbf{c}^{(0)} = 1 \tag{20}$$

By the similar derivation as TDes, the optimal weight of TRTap can be obtained, that is,

$$\widehat{\mathbf{w}}_{\mathrm{o}} = \widehat{\varphi}^{-1}\mathbf{A}\widetilde{\mathbf{F}}_m\mathbf{c}^{(0)}\left[(\mathbf{c}^{(0)})^{\mathrm{H}}\widetilde{\mathbf{F}}_m^{\mathrm{H}}\mathbf{A}^{\mathrm{H}}\widehat{\varphi}^{-1}\mathbf{A}\widetilde{\mathbf{F}}_m\mathbf{c}^{(0)}\right]^{-1}. \tag{21}$$

The summary of the computation of TRTap is similar as TDes, expect that $\widetilde{\mathbf{F}}_m$ is replaced by $\mathbf{A}\widetilde{\mathbf{F}}_m$.

4 Performance analyses

In the following, the optimal solutions of two proposed receivers are derived and compared. The MSE is defined as

$$E\left[|d_m^{(0)} - y|^2\right] \tag{22}$$

where $d_m^{(0)}$ is the desired signal and y is the adaptive filter's output. It is worthy to note that the MSE is only used for analyzing and comparing the system performance, not used for updating the filter's weight. The Geometric Series Formulas (GSF) is often applied in this section and in the appendices.

4.1 Optimal solution of TDes

The optimal solution of TDes receiver is obtained by calculating steady-state MSE with the optimal weight $\mathbf{w}_o$ as (16). The steady-state MSE of TDes is

$$\begin{aligned} J_o &= E\left[|d_m^{(0)} - \mathbf{w}^H(n)\widetilde{\mathbf{r}}_m|^2\right]|_{\mathbf{w}(n)=\mathbf{w}_o} \\ &= \sigma_d^2 - 2E\left[d_m^{(0)}\widetilde{\mathbf{r}}_m^H\right]\mathbf{w}_o + \mathbf{w}_o^H E\left[\widetilde{\mathbf{r}}_m\widetilde{\mathbf{r}}_m^H\right]\mathbf{w}_o \end{aligned}$$

where σ_d^2 is the energy of desired signal and $\sigma_d^2 = 1$ for PSK signal. From (9), we can derive $E\left[d_m^{(0)}\widetilde{\mathbf{r}}_m^H\right] = (\mathbf{c}^{(0)})^H\widetilde{\mathbf{F}}_m^H$, and then obtain $E\left[d_m^{(0)}\widetilde{\mathbf{r}}_m^H\right]\mathbf{w}_o = 1$. In addition, according to (9), the autocorrelation matrix of $\widetilde{\mathbf{r}}_m$ can be gained as

$$\varphi = E\left[\widetilde{\mathbf{r}}_m\widetilde{\mathbf{r}}_m^H\right] = \widetilde{\mathbf{F}}_m\mathbf{C}\mathbf{C}^H\widetilde{\mathbf{F}}_m^H + \sigma_n^2\mathbf{I} \tag{23}$$

where the fact that $E\left[\mathbf{F}_m\mathbf{g}(n)\mathbf{g}^H(n)\mathbf{F}_m^H\right] = \sigma_n^2\mathbf{F}_m\mathbf{F}_m^H = \sigma_n^2\mathbf{I}$ is used and σ_n^2 is the noise's variance. According to (23) and (16), we can obtain

$$\mathbf{w}_o^H\varphi\mathbf{w}_o = \left[(\mathbf{c}^{(0)})^H\widetilde{\mathbf{F}}_m^H\varphi^{-1}\widetilde{\mathbf{F}}_m\mathbf{c}^{(0)}\right]^{-1}. \tag{24}$$

Therefore, the steady-state MSE of TDes can be expressed as

$$J_o = \left[(\mathbf{c}^{(0)})^H\widetilde{\mathbf{F}}_m^H\varphi^{-1}\widetilde{\mathbf{F}}_m\mathbf{c}^{(0)}\right]^{-1} - 1. \tag{25}$$

4.2 Optimal solution of TRTap

Following the similar procedure for deriving the steady-state MSE of TDes, the optimal solution of TRTap can be acquired in terms of calculating steady-state MSE using the optimal weight $\widehat{\mathbf{w}}_o$ as (21). The steady-state MSE of TRTap is expressed as

$$\widehat{J}_o = \sigma_d^2 - 2E\left[d_m^{(0)}\widetilde{\mathbf{r}}_m^H\right]\mathbf{A}^H\widehat{\mathbf{w}}_o + \widehat{\mathbf{w}}_o^H\mathbf{A}E\left[\widetilde{\mathbf{r}}_m\widetilde{\mathbf{r}}_m^H\right]\mathbf{A}^H\widehat{\mathbf{w}}_o.$$

Due to $E\left[d_m^{(0)}\widetilde{\mathbf{r}}_m^H\right] = (\mathbf{c}^{(0)})^H\widetilde{\mathbf{F}}_m^H$, we obtain $E\left[d_m^{(0)}\widetilde{\mathbf{r}}_m^H\right]\mathbf{A}^H\widehat{\mathbf{w}}_o = 1$. Similar to (23), the autocorrelation matrix can be expressed as

$$\begin{aligned} \widehat{\varphi} &= \mathbf{A}E\left[\widetilde{\mathbf{r}}_m\widetilde{\mathbf{r}}_m^H\right]\mathbf{A}^H = \mathbf{A}\widetilde{\mathbf{F}}_m\mathbf{C}\mathbf{C}^H\widetilde{\mathbf{F}}_m^H\mathbf{A}^H + \sigma_n^2\mathbf{A}\mathbf{A}^H \\ &= \mathbf{A}\widetilde{\mathbf{F}}_m\mathbf{C}\mathbf{C}^H\widetilde{\mathbf{F}}_m^H\mathbf{A}^H + \sigma_n^2\mathbf{I} \end{aligned} \tag{26}$$

where the property of $\mathbf{A}\mathbf{A}^H = \mathbf{I}$ (derived in Appendix 2) is applied when $z \le N_c/\varsigma$. It is worthy to mention that in the case of $z > N_c/\varsigma$, $\mathbf{A}\mathbf{A}^H \neq \mathbf{I}$ is confirmed and then the noise terms will influence the desired signals. From (26) and (21), the steady-state MSE of TRTap thus can be obtained as

$$\widehat{J}_o = \left[(\mathbf{c}^{(0)})^H\widetilde{\mathbf{F}}_m^H\mathbf{A}^H\widehat{\varphi}^{-1}\mathbf{A}\widetilde{\mathbf{F}}_m\mathbf{c}^{(0)}\right]^{-1} - 1. \tag{27}$$

4.3 Performance comparisons

To compare the computational complexity, we show the requirement of complex multiplications of the proposed receivers in Appendix 4. Based on the property of $\widetilde{\mathbf{F}}_m$ which is derived in Appendix 5, the steady-state MSEs of both TDes and TRTap under two special environments are discussed in the following.

4.3.1 Multiple access scenario under AWGN channel

At first, the steady-state MSE of TDes is derived. According to the assumption of using orthogonal codes and AWGN channel, we have the multiplication $\mathbf{C}^H\mathbf{C} = \mathbf{I}$ and the channel matrix $\mathbf{H} = \mathbf{I}$. Consequently, $\widetilde{\mathbf{F}}_m$ becomes an identity matrix and the autocorrelation matrix φ in (23) can be expressed as $\mathbf{C}\mathbf{C}^H + \sigma_n^2\mathbf{I}$. The inverse matrix of φ can be derived further by matrix inversion lemma (MIL) [38]:

$$\begin{aligned} \varphi^{-1} &= \sigma_n^{-2}\mathbf{I} - \sigma_n^{-4}\mathbf{C}\left[\sigma_n^{-2}\mathbf{C}^H\mathbf{C} + \mathbf{I}\right]^{-1}\mathbf{C}^H \\ &= \sigma_n^{-2}\mathbf{I} - \frac{\sigma_n^{-4}}{\sigma_n^{-2}+1}\mathbf{C}\mathbf{C}^H \end{aligned}$$

where the second equality uses the result of $\mathbf{C}^H\mathbf{C} = \mathbf{I}$. The steady-state MSE of TDes in (25) can be written as

$$\begin{aligned} J_1 &= \left[\sigma_n^{-2}\mathbf{I} - \frac{\sigma_n^{-4}}{\sigma_n^{-2}+1}(\mathbf{c}^{(0)})^H\mathbf{C}\mathbf{C}^H\mathbf{c}^{(0)}\right]^{-1} - 1 \\ &= \left[\sigma_n^{-2}\mathbf{I} - \frac{\sigma_n^{-4}}{\sigma_n^{-2}+1}\right]^{-1} - 1 \\ &= \sigma_n^2 \end{aligned} \tag{28}$$

where the second equality uses the property of $(\mathbf{c}^{(0)})^H\mathbf{C} = [1, 0, \cdots, 0]$ due to applying orthogonal codes.

We can obtain the autocorrelation matrix of TRTap $\widehat{\varphi}$ as $\mathbf{A}\mathbf{C}\mathbf{C}^H\mathbf{A}^H + \sigma_n^2\mathbf{I}$. To calculate the steady-state MSE of TRTap, we consider two specific cases of $z = 1$ and $z = N_c/\varsigma$ shown below.

In case of $z = 1$, we have $\mathbf{A} = (\mathbf{c}^{(0)})^H$ shown in Appendix 3 and $\widehat{\varphi} = 1 + \sigma_n^2$. The steady-state MSE of TRTap with $z = 1$ becomes

$$\begin{aligned} \widehat{J}_1' &= (1+\sigma_n^2)/\left[(\mathbf{c}^{(0)})^H\widetilde{\mathbf{F}}_m^H\mathbf{A}^H\mathbf{A}\widetilde{\mathbf{F}}_m\mathbf{c}^{(0)}\right] - 1. \\ &= \sigma_n^2 \end{aligned} \tag{29}$$

As TRTap with $z = N_c/\varsigma$ is discussed, on the other hand, the inverse matrix of $\widehat{\varphi}$ can be derived as

$$\widehat{\varphi}^{-1} = \sigma_n^{-2}\mathbf{I} - \sigma_n^{-4}\mathbf{AC}\left[\sigma_n^{-2}\mathbf{C}^{\mathrm{H}}\mathbf{A}^{\mathrm{H}}\mathbf{AC} + \mathbf{I}\right]^{-1}\mathbf{C}^{\mathrm{H}}\mathbf{A}^{\mathrm{H}}$$

After applying the property of $\mathbf{A}^{\mathrm{H}}\mathbf{A} = \mathbf{I}$, we can rewrite $\widehat{\varphi}^{-1}$ as

$$\widehat{\varphi}^{-1} = \sigma_n^{-2}\mathbf{I} - \frac{\sigma_n^{-4}}{\sigma_n^{-2}+1}\mathbf{ACC}^{\mathrm{H}}\mathbf{A}^{\mathrm{H}}.$$

Therefore, the steady-state MSE of TRTap with $z = N_c/\varsigma$ is

$$\begin{aligned}\widehat{J}_1 &= \left[\sigma_n^{-2}\mathbf{I} - \frac{\sigma_n^{-4}}{\sigma_n^{-2}+1}(\mathbf{c}^{(0)})^{\mathrm{H}}\mathbf{A}^{\mathrm{H}}\mathbf{ACC}^{\mathrm{H}}\mathbf{A}^{\mathrm{H}}\mathbf{Ac}^{(0)}\right]^{-1} - 1 \\ &= \left[\sigma_n^{-2}\mathbf{I} - \frac{\sigma_n^{-4}}{\sigma_n^{-2}+1}\right]^{-1} - 1 \\ &= \sigma_n^2\end{aligned} \tag{30}$$

where the property of $(\mathbf{c}^{(0)})^{\mathrm{H}}\mathbf{A}^{\mathrm{H}}\mathbf{AC} = (\mathbf{c}^{(0)})^{\mathrm{H}}\mathbf{C}$ is applied in the second equality. When a set of orthogonal codes is applied in the proposed system in the presence of AWGN channel, we conclude as follows: (1) The steady-state MSE of TDes is equal to that of TRTap based on (28) and (29). (2) The increase of the number of taps used in TRTap receiver cannot upgrade the system performance because the proposed receiver with $z = 1$ can provide the best performance.

4.3.2 Single-user scenario under multipath fading channel

In this case, the steady-state MSE of TDes is evaluated at first. From (23) and using MIL, the inverse matrix of φ can be derived as

$$\begin{aligned}\varphi^{-1} &= \sigma_n^{-2}\mathbf{I} - \sigma_n^{-4}\widetilde{\mathbf{F}}_m\mathbf{c}^{(0)}\left[\sigma_n^{-2}(\mathbf{c}^{(0)})^{\mathrm{H}}\widetilde{\mathbf{F}}_m^{\mathrm{H}}\widetilde{\mathbf{F}}_m\mathbf{c}^{(0)} + \mathbf{I}\right]^{-1} \\ &\quad\times(\mathbf{c}^{(0)})^{\mathrm{H}}\widetilde{\mathbf{F}}_m^{\mathrm{H}} \\ &= \sigma_n^{-2}\mathbf{I} - \sigma_n^{-4}\widetilde{\mathbf{F}}_m\mathbf{c}^{(0)}(\mathbf{c}^{(0)})^{\mathrm{H}}\widetilde{\mathbf{F}}_m^{\mathrm{H}}/(\sigma_n^{-2}\alpha+1)\end{aligned}$$

where α is defined below (13), i.e., $\alpha = (\mathbf{c}^{(0)})^{\mathrm{H}}\widetilde{\mathbf{F}}_m^{\mathrm{H}}\widetilde{\mathbf{F}}_m\mathbf{c}^{(0)}$. Substituting the above equation into (24) and applying MIL again, we acquire

$$\begin{aligned}&\left[(\mathbf{c}^{(0)})^{\mathrm{H}}\widetilde{\mathbf{F}}_m^{\mathrm{H}}\varphi^{-1}\widetilde{\mathbf{F}}_m\mathbf{c}^{(0)}\right]^{-1} \\ &= \left[\sigma_n^{-2}\alpha - \sigma_n^{-4}(\mathbf{c}^{(0)})^{\mathrm{H}}\widetilde{\mathbf{F}}_m^{\mathrm{H}}\widetilde{\mathbf{F}}_m\mathbf{c}^{(0)}\right. \\ &\quad\left.\times(\mathbf{c}^{(0)})^{\mathrm{H}}\widetilde{\mathbf{F}}_m^{\mathrm{H}}\widetilde{\mathbf{F}}_m\mathbf{c}^{(0)}/(\sigma_n^{-2}\alpha+1)\right]^{-1} \\ &= (\sigma_n^{-2}\alpha+1)/(\sigma_n^{-2}\alpha)\end{aligned}$$

Consequently, the steady-state MSE of TDes becomes

$$J_2 = \frac{(\sigma_n^{-2}\alpha+1)}{\sigma_n^{-2}\alpha} - 1 = \sigma_n^2/\alpha. \tag{31}$$

Next, the steady-state MSE of TRTap is computed. The inverse matrix of $\widehat{\varphi}$ can be derived as

$$\widehat{\varphi}^{-1} = \sigma_n^{-2}\mathbf{I} - \sigma_n^{-4}\mathbf{A}\widetilde{\mathbf{F}}_{\mathbf{m}}\mathbf{c}^{(0)}(\mathbf{c}^{(0)})^{\mathrm{H}}\widetilde{\mathbf{F}}_m^{\mathrm{H}}\mathbf{A}^{\mathrm{H}}/(\sigma_n^{-2}\widehat{\alpha}+1)$$

where $\widehat{\alpha} = (\mathbf{c}^{(0)})^{\mathrm{H}}\widetilde{\mathbf{F}}_m^{\mathrm{H}}\mathbf{A}^{\mathrm{H}}\mathbf{A}\widetilde{\mathbf{F}}_m\mathbf{c}^{(0)}$. Following the similar mathematical derivation as TDes, the steady-state MSE of TRTap is obtained as $\sigma_n^2/\widehat{\alpha}$. Two cases of $z = 1$ and $z = N_c/\varsigma$ are also examined. In the case of $z = 1$, the result of $\mathbf{A}^{\mathrm{H}}\mathbf{A} = \mathbf{c}^{(0)}(\mathbf{c}^{(0)})^{\mathrm{H}}$ is shown in Appendix 3. Therefore, $\widehat{\alpha}$ becomes $(\mathbf{c}^{(0)})^{\mathrm{H}}\widetilde{\mathbf{F}}_m^{\mathrm{H}}\mathbf{c}^{(0)}(\mathbf{c}^{(0)})^{\mathrm{H}}\widetilde{\mathbf{F}}_m\mathbf{c}^{(0)}$. From (49), the steady-state MSE of TRTap with $z = 1$ can be given as

$$\widehat{J}_2' = \sigma_n^2/|h_0|^2. \tag{32}$$

In case of $z = N_c/\varsigma$, from (44), we have $\widehat{\alpha} = \alpha$. Consequently, the steady-state MSE of TRTap for $z = N_c/\varsigma$ becomes

$$\widehat{J}_2 = \sigma_n^2/\alpha. \tag{33}$$

According to (31) and (33), the steady-state MSE of TDes is equal to that of TRTap with $z = N_c/\varsigma$ in the single-user environment. From (32), (33), and (47), we have

$$\frac{\widehat{J}_2'}{\widehat{J}_2} = \frac{\sum_{l=0}^{N_p-1}|h_l|^2}{|h_0|^2}.$$

As expected, the TRTap receiver with $z = N_c/\varsigma$ can provide a better performance than that with $z = 1$.

5 Simulation results

This section provides several computer simulations and numerical results that demonstrate the performances of the proposed CM-based MC-CDMA receivers in two specific multipath fading channels. Channel 1 is a two-path channel and modeled as in [39], i.e., $\mathbf{h}_1 = \left[-0.1581 + 0.2841j, -0.1303 - 1.2193j\right]$. Channel 2 is a four-path channel and modeled as in [40], i.e., $\mathbf{h}_2 = \left[1.2, -1.2, 0.7j, -0.7j\right]$. Quadrature phase-shift keying (QPSK) modulation is employed in Figures 2, 3, 4, 5, 6, 7, 8, and QAM is adopted in Figure 9. Except for Figure 8, the system parameters $N_c = 128$ and $\varsigma = 2$ are used. In addition, the Walsh-Hadamard codes of length 64 and pseudonoise (PN) code of length 63 are adopted. A zero is padded right after the last chip of the PN codes to make the chip-size equal to the power of 2.

In Figure 2, by averaging over 300 independent trials, we compare the MSE learning curves of two proposed receivers using 63-chip PN codes operated at signal-to-noise ratio (SNR) = 20 dB, where the MSE is defined in (22). To fairly compare the performances of TRTap and

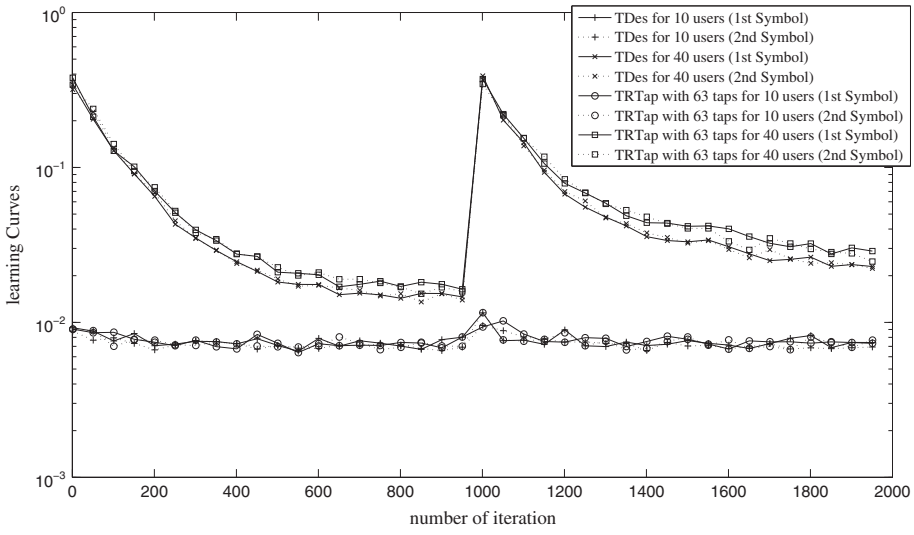

Figure 2 The MSE learning curves of the proposed receivers at SNR = 20 dB.

TDes, we set the tap length of TRTap as $z = 63$. In addition, to demonstrate the tracking capabilities of the proposed receivers, the multipath fading gains used are deliberately changed at the 1,000th symbol in the simulation. In high MAI environment (i.e., $K = 40$), the steady-state MSEs of TDes are lower than those of TRTap. However, the steady-state MSEs of TRTap can approach those of TRTap in the low MAI scenario (i.e., $K = 10$). Furthermore, we can verify that our proposed receivers can converge rapidly in a low-interference environment. From these learning curves, two QPSK symbols within the same OFDM symbol block are shown to provide similar convergence behaviors. Therefore, the only first QPSK symbol is considered and presented in the following simulations.

The SER performances for different number of active users are shown in Figure 3, where the 64-chips Hadamard codes are employed and $E_b/N_0 = 10$ dB. Considering the case of channel 1, the one-tap TRTap can offer fine SER performance as the number of users is small. In the case of channel 2, the SER performance of one-tap TRTap becomes worse even though the number of users is small. In addition, the degradations of the SER performances in channel 2 are obviously larger than those in channel 1. The

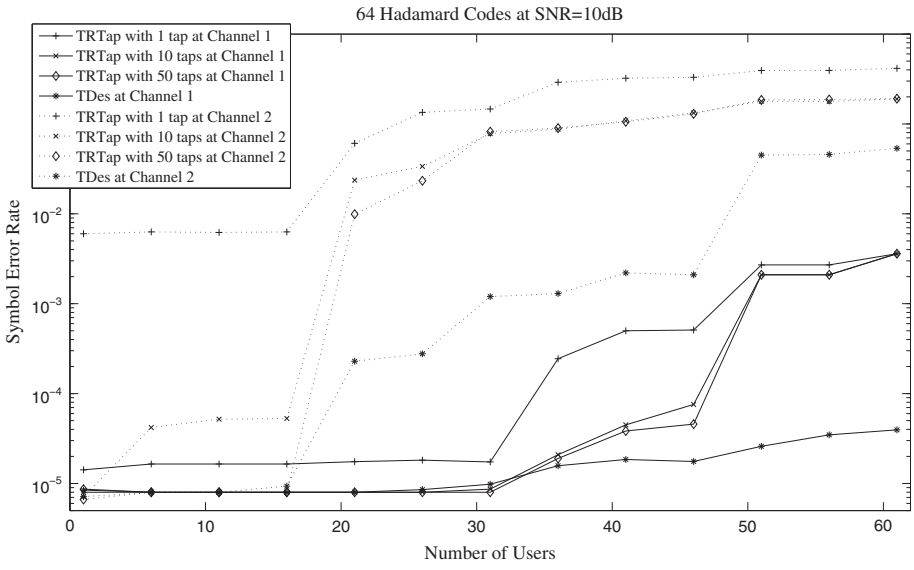

Figure 3 SER vs. the number of users for the proposed receivers at SNR = 10 dB.

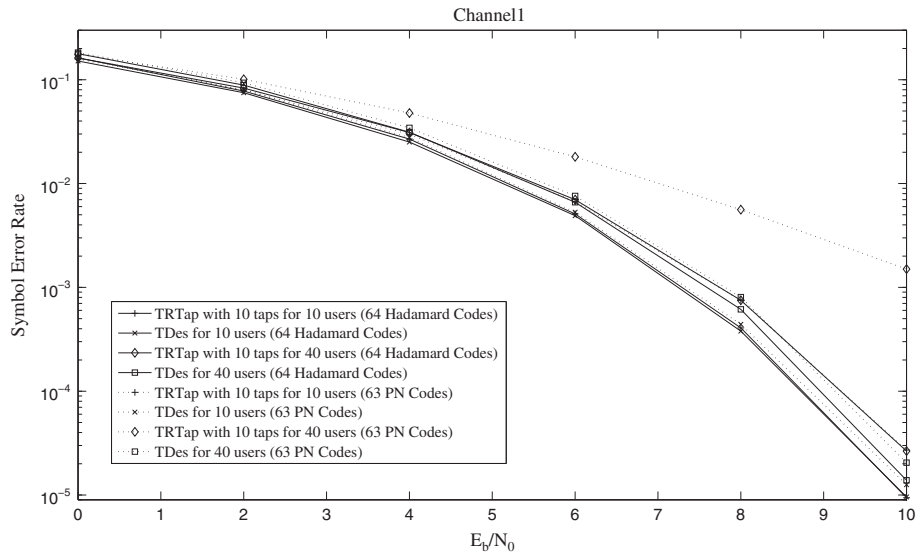

Figure 4 SER vs. E_b/N_0 for the proposed receivers at channel 1.

reason is that channel 2 causes larger ICI than channel 1. Accordingly, we can confirm that the one-tap TRTap performs well in low-interference environment, yet TDes is still necessary to be implemented in high MAI to achieve good performance.

As observed from Figure 4, TRTap can achieve similar SER performance as TDes when Hadamard codes are used. However, TRTap cannot perform well when PN codes are adopted and the number of users becomes larger. The reason is that in a large number of active users, TRTap with PN codes is more sensitive to MAIs than that with Hadamard codes.

The steady-state MSE performances of the proposed receivers using 63 PN codes under the AWGN and the multipath channels are illustrated in Figures 5 and 6, respectively. From Figure 5, without considering the effect of the multipath channel, the steady-state MSEs of TRTap receivers with the shortened tap (10 taps) and full tap (63 taps) are shown to be equivalent as those of TDes, and these simulation results of the steady-state MSEs are consistent with the analytical MSE results derived in Section 4.3.1. On the other hand, in the presence of the multipath channel (in channel 1), Figure 6 shows that TDes has similar steady-state MSE performance as that of

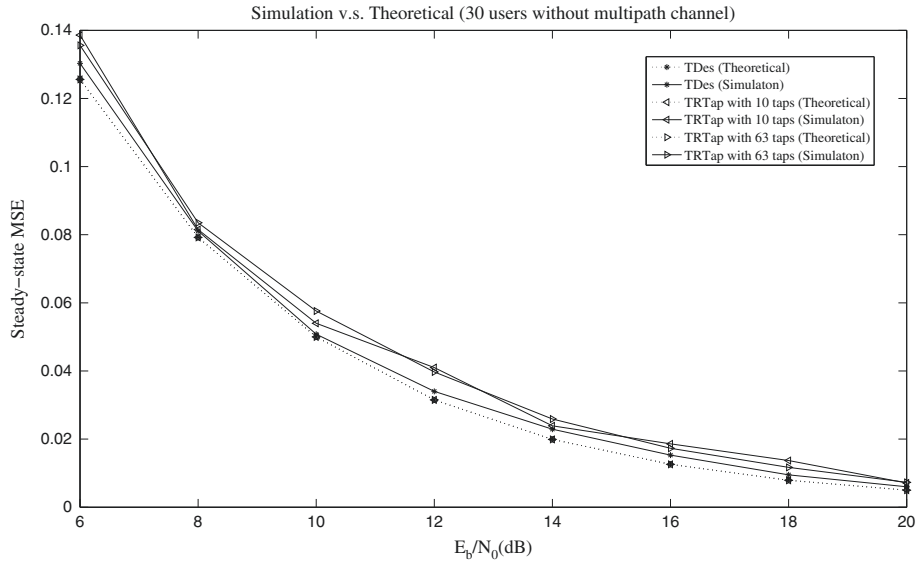

Figure 5 Theoretical and simulated steady-state MSE comparisons for the proposed receivers without multipath channel.

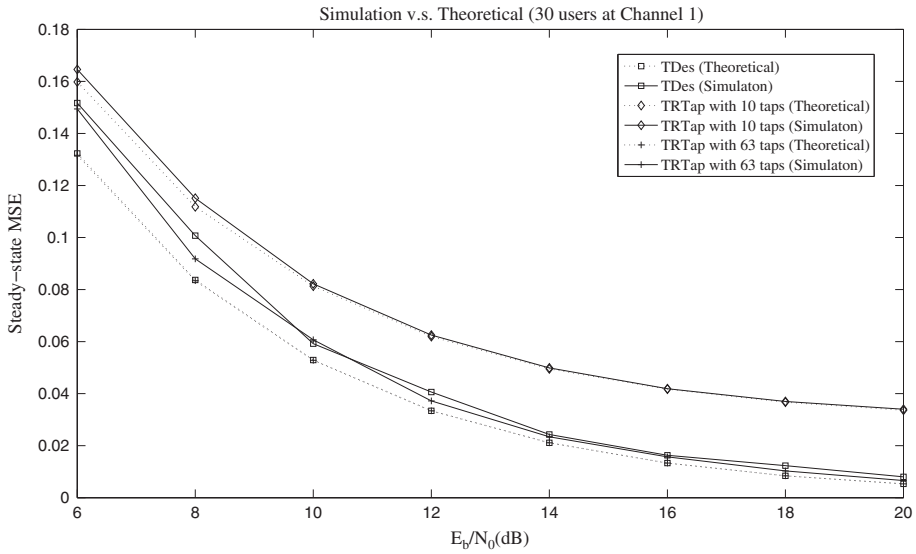

Figure 6 Theoretical and simulated steady-state MSE comparisons for the proposed receivers at channel 1.

full-tap TRTap yet provides the better steady-state MSE performance compared with ten-tap TRTap; this outcome coincides with the results derived in Section 4.3.2. Besides, the misadjustment of steepest-descent method in [41] is proportional to total tap-input power, thus it can be anticipated that the discrepancy of the steady-state MSE between theoretical results and simulation results in higher SNR is less than that in lower SNR. As expected, Figure 6 indicates that the theoretical results are close to simulation results in higher SNR. Furthermore, TRTap using the larger number of taps results in a great mismatch between analytical and simulation results of the steady-state MSE, in which this trend also corresponds to the inference in [41].

The impact of the channel estimation's error on the system performance is investigated in Figure 7. Following [5], we compare the SERs of the proposed receivers with respect to the variance of the channel estimation's error. The error of the channel estimation is defined as the difference between the estimated channel and the simulated channel (i.e., the channel really used in the simulation). As the number of users is small (i.e., in cases of low MAI), both proposed TDes and TRTap receivers perform well and achieve almost the same SER perfor-

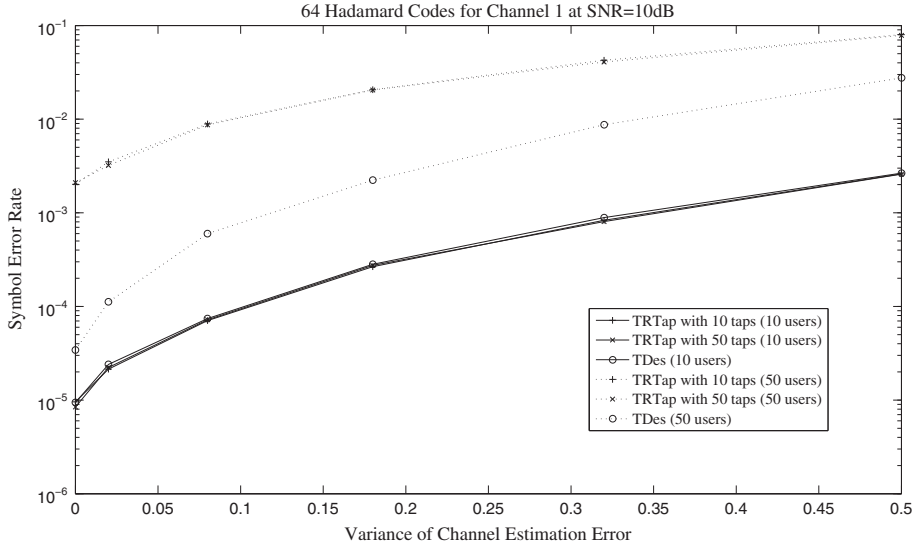

Figure 7 SER vs. variance of channel estimation error for the proposed receivers.

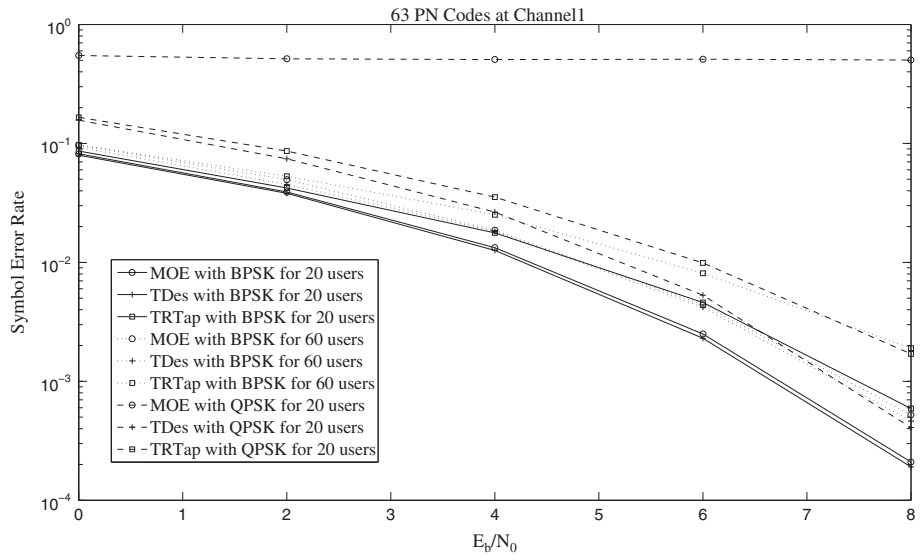

Figure 8 SER comparisons of the proposed receivers and MOE at channel 1.

mance even if the variance of the channel estimation's error is large. However, in high MAI environment, the SER performance of TDes is better than that of TRTap which is still bad in the range of low channel estimation error. It is concluded that increasing the number of tap is not able to improve the capability of TRTap receiver against the channel estimation error.

Figure 8 shows the SER performances among TDes, TRTap, and the constrained MOE receiver proposed in [21]. The downlink environment is considered, and the binary phase-shift keying (BPSK) and QPSK modulations are adopted in all systems under investigation. To obtain the fair performance comparison, we select $N_c = 64$ and $\varsigma = 1$ in both the TDes and TRTap receivers because the constrained MOE receiver only provides the detection for the single-symbol transmission [21]. By using the BPSK modulation, the SER performance of TDes is similar to that of MOE, and the SER of TRTap can approach that of MOE when the number of users is large. In addition, both TDes and TRTap receivers can perform well when the QPSK modulation is applied in the examined systems. However, the performance of MOE receiver in the QPSK-modulated system becomes worse because the MOE receiver is originally designed to handle the real-valued modulation such as BPSK. Finally, we simulate

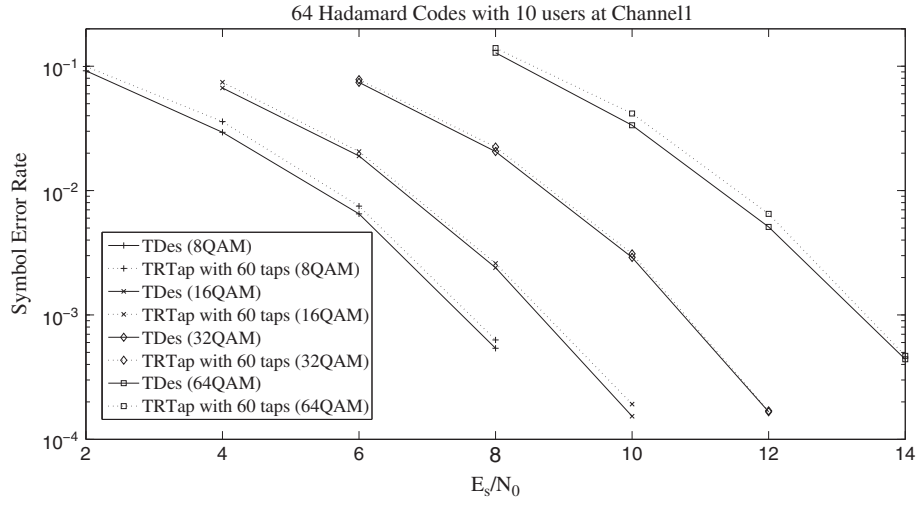

Figure 9 SER vs. E_s/N_0 for the proposed receivers with QAM at channel 1.

the proposed receivers by M-ary QAM. As the modulation level M increases, the system performances of the proposed receivers degrade obviously. Besides, the 60-tap TRTap can achieve the similar SER performance as TDes for every M-ary QAM.

6 Conclusions

Two blind adaptive MC-CDMA receivers are proposed in this paper. In order to guarantee the global convergence, the proposed receivers adopt the constrained CM-based algorithms to realize the transmission of multiple date symbols within one OFDM block. The fixed-length (TDes) and variable-length (TRTap) receivers are derived and analyzed as the length of CP is longer than the delay spread of the multipath channel. The advantage of the TDes is that it can provide a better SER performance than TRTap in severe interference environment. However, the tap length of the TDes has to be equal to the code length of the spreading codes. In contrast, the TRTap receiver has a high degree of freedom to offer the trade-off between the performance and the complexity. The TRTap can achieve similar steady-state MSE as TDes in low interference environment even if the TRTap adopts only one-tap equalization. Simulations are also compared with the theoretical results to verify the correctness of the mathematical derivation.

Appendix 1

Properties of $\mathbf{F}_m$

In this appendix, two properties of $\mathbf{F}_m$, i.e., $\mathbf{F}_m\mathbf{F}_m^{\mathrm{H}} = \mathbf{I}$ and $\mathbf{F}_m^{\mathrm{H}}\mathbf{F}_m \neq \mathbf{I}$, are presented in the following. At first, based on (5), the multiplication of $\mathbf{F}_m$ and $\mathbf{F}_m^{\mathrm{H}}$ becomes a $(N_c/\varsigma) \times (N_c/\varsigma)$ matrix with (r,s)th element

$$\begin{aligned} f'_{r,s} &= \frac{1}{N_c}\sum_{p=0}^{N_c-1} w^{p\times(m+r\varsigma)}(w^{p\times(m+s\varsigma)})^* \\ &= \frac{1}{N_c}\sum_{p=0}^{N_c-1} e^{j\frac{2\pi}{N_c}(s-r)\varsigma p} \\ &= \begin{cases} 1; & r=s \\ 0; & \text{others} \end{cases} \end{aligned} \tag{34}$$

where GSF is applied to obtain the last equality of the above equation. Hence, we have $\mathbf{F}_m\mathbf{F}_m^{\mathrm{H}} = \mathbf{I}$. Secondly, the multiplication of $\mathbf{F}_m^{\mathrm{H}}$ and $\mathbf{F}_m$ becomes a $N_c \times N_c$ matrix with (r,s)th element

$$f''_{r,s} = \frac{1}{N_c}\sum_{p=0}^{N_c/\varsigma-1} e^{j\frac{2\pi}{N_c}(r-s)(m+\varsigma p)}. \tag{35}$$

We can show that $f''_{r,s} = 1/\varsigma$ if $r = s$ and

$$f''_{r,s} = \frac{1}{N_c}\frac{e^{j\frac{2\pi}{N_c}(r-s)m}(1-e^{j2\pi(r-s)})}{1-e^{j\frac{2\pi}{N_c}(r-s)\varsigma}} = \beta$$

if $r \neq s$. It is worthy to note that r and s are positive integers, and β can be 0 in most cases. However, when $r-s = \pm q(N_c/\varsigma)$, in the specific case, β becomes

$$\begin{aligned} \beta &= \frac{1}{N_c}\frac{e^{\pm j2\pi(m/\varsigma)q}(1-e^{\pm j2\pi(N_c/\varsigma)q})}{1-e^{\pm j2\pi q}} \\ &= \frac{1}{N_c}\frac{e^{\pm j2\pi(m/\varsigma)q}(1-\cos(2\pi(N_c/\varsigma)q)\mp j\sin(2\pi(N_c/\varsigma)q))}{1-\cos(2\pi q)\mp j\sin(2\pi q)} \end{aligned}$$

where $q \in \{1,\cdots,\varsigma-1\}$. Since ς, N_c, and N_c/ς are the powers of 2 and m is a non-negative integer, β can be further reduced as

$$\beta = \frac{1}{N_c}\frac{e^{\pm j2\pi(m/\varsigma)q}(\sin(2\pi(N_c/\varsigma)q))}{\sin(2\pi q)}.$$

In terms of using the trigonometric functions, $\sin(2\pi(N_c/\varsigma)q) = 2\sin(2\pi(N_c/(2\varsigma))q)\cos(2\pi(N_c/(2\varsigma))q)$, we acquire

$$\begin{aligned} \frac{\sin(2\pi(N_c/\varsigma)q)}{\sin(2\pi q)} &= \frac{(N_c/\varsigma)\sin(2\pi q)\prod_{p=0}^{\log_2(N_c/\varsigma)-1}\cos(2\pi q 2^p)}{\sin(2\pi q)} \\ &= N_c/\varsigma. \end{aligned} \tag{36}$$

Therefore, $\beta = \frac{1}{\varsigma}e^{\pm j2\pi(m/\varsigma)q}$ when $r-s = \pm q(N_c/\varsigma)$. To summarize, the (r,s)th element of $\mathbf{F}_m^{\mathrm{H}}\mathbf{F}_m$ becomes

$$f''_{r,s} = \begin{cases} 1/\varsigma & r=s \\ \frac{1}{\varsigma}e^{j2\pi(m/N_c)(r-s)}; & r-s=\pm q(N_c/\varsigma) \\ 0; & \text{others} \end{cases} \tag{37}$$

where $q \in \{1,\cdots,\varsigma-1\}$. Accordingly, we have $\mathbf{F}_m^{\mathrm{H}}\mathbf{F}_m \neq \mathbf{I}$.

Appendix 2

Multiplication of A and $\mathbf{A}^{\mathrm{H}}$

From (19), the (i',j')th element of $\mathbf{A}\mathbf{A}^{\mathrm{H}}$ can be written as

$$a_{i',j'} = (\mathbf{c}^{(0)})^{\mathrm{H}}\mathbf{F}_m\mathbf{I}_{i'}^{\mathrm{H}}\mathbf{F}_m^{\mathrm{H}}\mathbf{F}_m\mathbf{I}_{j'}\mathbf{F}_m^{\mathrm{H}}\mathbf{c}^{(0)}. \tag{38}$$

First, we derive the result of $\mathbf{I}_{i'}^{\mathrm{H}}\mathbf{F}_m^{\mathrm{H}}\mathbf{F}_m\mathbf{I}_{j'}$. Let the (r,s)th element of $\mathbf{I}_{i'}^{\mathrm{H}}\mathbf{F}_m^{\mathrm{H}}\mathbf{F}_m\mathbf{I}_{j'}$ is $f'''_{r,s}$. It is noted that $\mathbf{I}_{i'}^{\mathrm{H}}\mathbf{F}_m^{\mathrm{H}}\mathbf{F}_m\mathbf{I}_{j'}$ circularly shifts each elements of $\mathbf{F}_m^{\mathrm{H}}\mathbf{F}_m$ up by i' rows and left by j' columns. Therefore, from (37) and (7), we have $f'''_{r,s} = f''_{r',s'}$, where $r' = \mathrm{mod}_{N_c}(r+i')$, $s' = \mathrm{mod}_{N_c}(s+j')$, $f''_{r',s'}$ is defined in (37) and mod denote the modulus operation.

After carrying out circularly shift, $f'''_{r,s}$ can be expressed as

$$f'''_{r,s}=\begin{cases}(1/\varsigma)e^{j2\pi(m/N_c)(r+i'-(s+j'))}; & \text{if } r+i'-(s+j')=\pm q'(N_c/\varsigma)\\ 0; & \text{others}\end{cases}$$

where q' is an arbitrary integer. Based on above equation, the(α',β')th element of $\mathbf{F}_m\mathbf{I}_{i'}^{\mathrm{H}}\mathbf{F}_m^{\mathrm{H}}\mathbf{F}_m\mathbf{I}_{j'}\mathbf{F}_m^{\mathrm{H}}$ is

$$\begin{aligned}f''''_{\alpha',\beta'} &= \sum_{s=0}^{N_c-1}\sum_{r=0}^{N_c-1} f'''_{r,s}e^{-j(2\pi/N_c)(m+\alpha'\varsigma)r}e^{j(2\pi/N_c)(m+\beta'\varsigma)s}\\ &= \frac{1}{N_c\varsigma}\sum_{s=0}^{N_c-1}\sum_{\varkappa=0}^{\varsigma-1} e^{-j2\pi\alpha'\varkappa}e^{-j2\pi(\varsigma/N_c)(\alpha'-\beta')s}\\ &\quad\times e^{j2\pi(\varsigma/N_c)\alpha'(i'-j')}e^{j(2\pi/N_c)m(i'-j')}\\ &= \frac{1}{N_c\varsigma}e^{j2\pi(\varsigma/N_c)\alpha'(i'-j')}e^{j(2\pi/N_c)m(i'-j')}\\ &\quad\times\sum_{s=0}^{N_c-1} e^{-j2\pi(\varsigma/N_c)(\alpha'-\beta')s}\sum_{\varkappa=0}^{\varsigma-1} e^{-j2\pi\alpha'\varkappa}\\ &= \frac{1}{N_c}e^{j2\pi(\varsigma/N_c)\alpha'(i'-j')}e^{j(2\pi/N_c)m(i'-j')}\\ &\quad\times\sum_{s=0}^{N_c-1} e^{-j2\pi(\varsigma/N_c)(\alpha'-\beta')s}\\ &= \begin{cases}e^{j2\pi(\varsigma/N_c)\alpha'(i'-j')}e^{j(2\pi/N_c)m(i'-j')}; & \text{if } \alpha'=\beta'\\ 0; & \text{others}\end{cases}\end{aligned} \tag{39}$$

where $\varkappa=(\varsigma/N_c)(r+i'-(s+j'))$. The fourth equality of (39) uses the result of $\sum_{\varkappa=0}^{\varsigma-1} e^{-j2\pi\alpha'\varkappa}=\varsigma$ which can be acquired in terms of the similar derivation of (36)). In addition, the fifth equality of (39) uses the identity that

$$\sum_{s=0}^{N_c-1} e^{-j2\pi(\varsigma/N_c)(\alpha'-\beta')s}=\begin{cases}N_c; & \text{if } \alpha'=\beta'\\ 0; & \text{others.}\end{cases}$$

Therefore, $\mathbf{F}_m\mathbf{I}_{i'}^{\mathrm{H}}\mathbf{F}_m^{\mathrm{H}}\mathbf{F}_m\mathbf{I}_{j'}\mathbf{F}_m^{\mathrm{H}}$ is a diagonal matrix. Specifically, $\mathbf{F}_m\mathbf{I}_{i'}^{\mathrm{H}}\mathbf{F}_m^{\mathrm{H}}\mathbf{F}_m\mathbf{I}_{j'}\mathbf{F}_m^{\mathrm{H}}$ becomes an identity matrix if $i'=j'$. According to (38) and

$$\mathbf{c}^{\mathrm{H}}\mathbf{S}\mathbf{c}=\sum_{r=0}^{N_c/\varsigma-1} c_r^2 s_{r,r}=\sum_{r=0}^{N_c/\varsigma-1} s_{r,r} \tag{40}$$

where $\mathbf{S}$ is a diagonal matrix, the (i',j')th element of $\mathbf{A}\mathbf{A}^{\mathrm{H}}$ can be obtained as

$$\begin{aligned}a_{i',j'} &= e^{j(2\pi/N_c)m(i'-j')}\sum_{r=0}^{N_c/\varsigma-1} e^{j2\pi(\varsigma/N_c)(i'-j')r}\\ &= \begin{cases}1; & \text{if } i'=j'\\ e^{j(2\pi/N_c)m(i'-j')}\frac{1-e^{j2\pi(i'-j')}}{1-e^{j2\pi(\varsigma/N_c)(i'-j')}}; & \text{if } i'-j'=q'(N_c/\varsigma)\\ 0; & \text{others}\end{cases}\end{aligned}$$

where q' is an arbitrary integer. From above equation, we can confirm that $\mathbf{A}\mathbf{A}^{\mathrm{H}}=\mathbf{I}$ as $z\le N_c/\varsigma$ and $\mathbf{A}\mathbf{A}^{\mathrm{H}}\neq\mathbf{I}$ as $z>N_c/\varsigma$.

Appendix 3

Multiplication of $\mathbf{A}^{\mathrm{H}}$ and $\mathbf{A}$

From (19), the multiplication of $\mathbf{A}^{\mathrm{H}}$ and $\mathbf{A}$ can be written as

$$\mathbf{A}^{\mathrm{H}}\mathbf{A}=\sum_{i'=0}^{z-1}\mathbf{F}_m\mathbf{I}_{i'}\mathbf{F}_m^{\mathrm{H}}\mathbf{c}^{(0)}(\mathbf{c}^{(0)})^{\mathrm{H}}\mathbf{F}_m\mathbf{I}_{i'}^{\mathrm{H}}\mathbf{F}_m^{\mathrm{H}}. \tag{41}$$

We discuss (41) in two special cases: $z=1$ and $z=N_c/\varsigma$. In case of $z=1$, the right-hand side of (41) becomes $\mathbf{F}_m\mathbf{I}\mathbf{F}_m^{\mathrm{H}}\mathbf{c}^{(0)}(\mathbf{c}^{(0)})^{\mathrm{H}}\mathbf{F}_m\mathbf{I}^{\mathrm{H}}\mathbf{F}_m^{\mathrm{H}}$. Thus, we obtain $\mathbf{A}^{\mathrm{H}}\mathbf{A}=\mathbf{c}^{(0)}(\mathbf{c}^{(0)})^{\mathrm{H}}$ as $z=1$. For the case of $z=N_c/\varsigma$, we firstly show that $\mathbf{F}_m\mathbf{I}_{i'}\mathbf{F}_m^{\mathrm{H}}$ is a diagonal matrix. Since $\mathbf{F}_m\mathbf{I}_{i'}$ circularly shifts each column vector of $\mathbf{F}_m$ left by i' columns, in terms of the circular shift property, the (r,s) th element of $\mathbf{F}_m\mathbf{I}_{i'}\mathbf{F}_m^{\mathrm{H}}$ is

$$\begin{aligned}&\frac{1}{N_c}\sum_{p=0}^{N_c-1} w^{(m+r\varsigma)(i'+p)}(w^{(m+s\varsigma)p})^*\\ &= e^{-j(2\pi/N_c)(m+r\varsigma)i'}\frac{1}{N_c}\sum_{p=0}^{N_c-1} e^{j(2\pi/N_c)(s-r)\varsigma p}\\ &= \begin{cases}e^{-j(2\pi/N_c)(m+r\varsigma)i'}; & \text{if } r=s\\ 0; & \text{others}\end{cases}\end{aligned} \tag{42}$$

By similar manipulation, the (r,s)th element of $\mathbf{F}_m\mathbf{I}_{i'}^{\mathrm{H}}\mathbf{F}_m^{\mathrm{H}}$ can be acquired as

$$\begin{cases}e^{j(2\pi/N_c)(m+r\varsigma)i'}; & \text{if } r=s\\ 0; & \text{others.}\end{cases} \tag{43}$$

To summarize, $\mathbf{F}_m\mathbf{I}_{i'}\mathbf{F}_m^{\mathrm{H}}$ and $\mathbf{F}_m\mathbf{I}_{i'}^{\mathrm{H}}\mathbf{F}_m^{\mathrm{H}}$ are all diagonal matrix. Consequently, the sth element of $(N_c/\varsigma)\times 1$ vector $(\mathbf{c}^{(0)})^{\mathrm{H}}\mathbf{F}_m\mathbf{I}_{i'}^{\mathrm{H}}\mathbf{F}_m^{\mathrm{H}}$ is $c_s^{(0)}e^{j(2\pi/N_c)(m+s\varsigma)i'}$ and the rth element of $\mathbf{F}_m\mathbf{I}_{i'}\mathbf{F}_m^{\mathrm{H}}\mathbf{c}^{(0)}$ is $c_r^{(0)}e^{-j(2\pi/N_c)(m+r\varsigma)i'}$, respectively Afterward, the (r,s)th element of $\mathbf{F}_m\mathbf{I}_{i'}\mathbf{F}_m^{\mathrm{H}}\mathbf{c}^{(0)}(\mathbf{c}^{(0)})^{\mathrm{H}}\mathbf{F}_m\mathbf{I}_{i'}^{\mathrm{H}}\mathbf{F}_m^{\mathrm{H}}$ is $c_r^{(0)}c_s^{(0)}e^{j(2\pi/N_c)(s-r)\varsigma i'}$. From (41), the (r,s)th element of $\mathbf{A}^{\mathrm{H}}\mathbf{A}$ can be written as

$$\begin{aligned}&c_r^{(0)}c_s^{(0)}\sum_{i'=0}^{N_c/\varsigma-1} e^{j(2\pi/N_c)(s-r)\varsigma i'}\\ &= \begin{cases}1; & \textit{if } r=s\\ 0; & \text{others.}\end{cases}\end{aligned} \tag{44}$$

Therefore, we obtain $\mathbf{A}^{\mathrm{H}}\mathbf{A}=\mathbf{I}$ when $z=N_c/\varsigma$.

Appendix 4

Computational complexity

Assume that the rate of channel changes is very low, and the channel state information is fixed in one period. Thus,

$\mathbf{w}_q$, $\mathbf{B}$ for TDes, and $\widehat{\mathbf{w}}_q$, $\widehat{\mathbf{B}}$ for TRTap can be regarded as fix portion in one period. At first, we show the requirement of complex multiplications of TDes. From the summary of Section 3.1, we can see that to produce $\mathbf{w}(n)$, y, φ, ε, and $\mathbf{w}_a(n+1)$ requires G^2, G, G^2, $2G^2$, and $1+G+G^3+G^2$ multiplications, respectively. Therefore, TDes requires totally $1+2G+4G^2+G^3$ multiplications in one iteration. Second, from the summary of Section 3.2, we can see that to produce $\mathbf{w}(n)$, $\mathbf{A}\widetilde{\mathbf{r}}_m$, y, φ, ε, and $\mathbf{w}_a(n+1)$ requires z^2, zG, z, z^2, $2z^2$, and $1+z+z^3+z^2$ multiplications, respectively. Therefore, TRTap requires totally $1+2z+4z^2+z^3+zG$ multiplications in one iteration. Since z can be smaller than G, the computational complexity of TRTap can be lower than that of TDes.

Appendix 5

Properties of $\widetilde{\mathbf{F}}_m$

At first, we show $\widetilde{\mathbf{F}}_m$ is a diagonal matrix. Due to

$$\widetilde{\mathbf{F}}_m = \mathbf{F}_m\mathbf{H}\mathbf{F}_m^{\mathrm{H}} = \mathbf{F}_m\Big(\sum_{l=0}^{N_P-1} h_l\mathbf{I}_l\Big)\mathbf{F}_m^{\mathrm{H}}$$

and from (42), the (r,s)th element of $\widetilde{\mathbf{F}}_m$ can be expressed as

$$\begin{cases} \sum_{l=0}^{N_P-1} h_l e^{-j(2\pi/N_c)(m+r\varsigma)l}; & \text{if } r=s \\ 0; & \text{others.} \end{cases} \tag{45}$$

Thus, $\widetilde{\mathbf{F}}_m^{\mathrm{H}}\widetilde{\mathbf{F}}_m$ is also a diagonal matrix whose (r,s)th element is

$$\begin{cases} \Big(\sum_{l_1=0}^{N_P-1} h_{l_1} e^{-j(2\pi/N_c)(m+r\varsigma)l_1}\Big)\Big(\sum_{l_2=0}^{N_P-1} h_{l_2}^* e^{j(2\pi/N_c)(m+r\varsigma)l_2}\Big); & \text{if } r=s \\ 0; & \text{others.} \end{cases} \tag{46}$$

Afterward, the results of the multiplications of two matrices, $(\mathbf{c}^{(0)})^{\mathrm{H}}\widetilde{\mathbf{F}}_m^{\mathrm{H}}\widetilde{\mathbf{F}}_m\mathbf{c}^{(0)}$ and $(\mathbf{c}^{(0)})^{\mathrm{H}}\widetilde{\mathbf{F}}_m^{\mathrm{H}}\mathbf{c}^{(0)}(\mathbf{c}^{(0)})^{\mathrm{H}}\widetilde{\mathbf{F}}_m\mathbf{c}^{(0)}$, are derived below. From (46) and (40), we can obtain

$$\begin{aligned} &(\mathbf{c}^{(0)})^{\mathrm{H}}\widetilde{\mathbf{F}}_m^{\mathrm{H}}\widetilde{\mathbf{F}}_m\mathbf{c}^{(0)} \\ &= \frac{\varsigma}{N_c}\sum_{l_1=0}^{N_P-1}\sum_{l_2=0}^{N_P-1} h_{l_1}h_{l_2}^* e^{j(2\pi/N_c)m(l_2-l_1)}\sum_{r=0}^{N_c/\varsigma-1} e^{j(2\pi/N_c)(l_2-l_1)\varsigma r} \\ &= \sum_{l=0}^{N_P-1}|h_l|^2 \end{aligned} \tag{47}$$

where the last equality of above equation applies the result of

$$\sum_{r=0}^{N_c/\varsigma-1} e^{j(2\pi/N_c)(l_2-l_1)\varsigma r} = \begin{cases} N_c/\varsigma; & \text{if } l_2=l_1 \\ 0; & \text{others.} \end{cases} \tag{48}$$

To compute the result of $(\mathbf{c}^{(0)})^{\mathrm{H}}\widetilde{\mathbf{F}}_m^{\mathrm{H}}\mathbf{c}^{(0)}(\mathbf{c}^{(0)})^{\mathrm{H}}\widetilde{\mathbf{F}}_m\mathbf{c}^{(0)}$, we first discuss the multiplication $(\mathbf{c}^{(0)})^{\mathrm{H}}\widetilde{\mathbf{F}}_m\mathbf{c}$. From (45) and (40), we can obtain

$$\begin{aligned} &(\mathbf{c}^{(0)})^{\mathrm{H}}\widetilde{\mathbf{F}}_m\mathbf{c}^{(0)} \\ &= \frac{\varsigma}{N_c}\sum_{l=0}^{N_P-1} h_l e^{-j(2\pi/N_c)ml}\sum_{r=0}^{N_c/\varsigma-1} e^{-j(2\pi/N_c)l\varsigma r} \\ &= h_0 \end{aligned}$$

where the last equality of above equation use the similar derivation of (48). Based on the result of above equation, accordingly, we have

$$(\mathbf{c}^{(0)})^{\mathrm{H}}\widetilde{\mathbf{F}}_m^{\mathrm{H}}\mathbf{c}^{(0)}(\mathbf{c}^{(0)})^{\mathrm{H}}\widetilde{\mathbf{F}}_m\mathbf{c}^{(0)} = |h_0|^2. \tag{49}$$

Competing interests
The authors declare that they have no competing interests.

Acknowledgements
This work was supported in part by the National Science Council of Taiwan under contract NSC 102-2221-E-150-030 and NSC 100-2221-E-228-002.

Author details
[1]Institute of Computer and Communication Engineering, Jinwen University of Science and Technology, Taipei 231-54, Taiwan. [2]Department of Aeronautical Engineering, National Formosa University, Huwei 632, Taiwan.

Received: 2 November 2012 Accepted: 19 November 2013
Published: 1 December 2013

References

1. S Hara, R Prasad, Overview of multicarrier CDMA. IEEE Commun. Mag. **35**, 126–133 (1997)
2. AC McCormick, EA Al-Susa, Multicarrier CDMA for future generation mobile communication. IEEE Electron Commun Eng J. **14**, 52–60 (2002)
3. L Mucchi, S Morosi, ED Re, R Fantacci, A new algorithm for blind adaptive multiuser detection in frequency selective multipath fading channel. IEEE Trans. Wireless Commun. **3**, 235–247 (2004)
4. X Wang, HV Poor, Blind adaptive multiuser detection in multipath CDMA channels based on subspace tracking. IEEE Trans. Signal Process. **46**, 3030–3044 (1998)
5. J Miguez, L Castedo, A linearly constrained constant modulus approach to blind adaptive multiuser interference suppression. IEEE Commun. Lett. **2**, 217–219 (1998)
6. C Xu, G Feng, Comments on "A linearly constrained constant modulus approach to blind adaptive multiuser interference suppression". IEEE Commun. Lett. **4**, 280–282 (2000)
7. C Xu, G Feng, KS Kwak, A modified constrained constant modulus approach to blind adaptive multiuser detection. IEEE Trans. Commun. **49**, 1642–1648 (2001)
8. JK Tugnait, T Li, Blind detection of asynchronous CDMA signals in multipath channels using code-constrained inverse filter criterion. IEEE Trans. Signal Process. **49**, 1300–1309 (2001)
9. Z Xu, P Liu, Code-constrained blind detection of CDMA signals in multipath channels. IEEE Sig. Proc. Lett. **9**, 389–392 (2002)
10. RC de Lamare, RS Neto, Blind adaptive code-constrained constant modulus algorithms for CDMA interference suppression in multipath channels. IEEE Commun. Lett. **9**, 334–336 (2005)
11. HH Zeng, L Tong, CR Johnson Jr, Relationships between the constant modulus and Wiener receivers. IEEE Trans. Inf. Theory. **44**, 1523–1538 (1998)
12. Z Xu, MK Tsatsanis, Blind adaptive algorithms for minimum variance CDMA receivers. IEEE Trans. Commun. **49**, 180–194 (2001)

13. FB Ueng, JD Chen, SC Tsai, PY Chen, Blind adaptive DS/CDMA receivers for multipath and multiuser environments. IEEE Trans. Circuits Syst. I: Fundam. Theory Appl. **53**, 440–453 (2006)
14. U Madhow, Blind adaptive interference suppression for direct-sequence CDMA. Proc. IEEE. **86**, 2049–2069 (1998)
15. B Hu, LL Yang, L Hanzo, Time- and frequency-domain-spread generalized multicarrier DS-CDMA using subspace-based blind and group-blind space–time multiuser detection. IEEE Trans. Vehicular Technol. **57**, 3235–3241 (2008)
16. F Verde, Subspace-based blind multiuser detection for quasi-synchronous MC-CDMA systems. IEEE Signal Process. Lett. **11**, 621–624 (2004)
17. DJ Sadler, A Manikas, Blind reception of multicarrier DS-CDMA using antenna arrays. IEEE Trans. Wireless Commun. **2**, 1231–1239 (2003)
18. G Zhang, G Bi, L Zhang, Blind multiuser detection for asynchronous MC-CDMA systems without channel estimation. IEEE Trans. Vehicular Technol. **47**, 1001–1013 (2004)
19. TM Lok, TF Wong, JS Lehnert, Blind adaptive signal reception for MC-CDMA systems in Rayleigh fading channels. IEEE Trans. Commun. **47**, 464–471 (1999)
20. A Djebbar, K Abed-Meraim, A Djebbari, Blind and semi-blind equalization of downlink MC-CDMA system exploiting guard interval redundancy and excess codes. IEEE Trans. Commun. **57**, 156–163 (2009)
21. B Seo, HM Kim, Blind adaptive constrained MOE receiver for uplink MC-CDMA systems with real signaling in multi-cell environments. IEEE Trans. Wireless Commun. **8**, 4911–4915 (2009)
22. H Cheng, SC Chan, Blind linear MMSE receivers for MC-CDMA systems. IEEE Trans. Circuits Syst. I: Regular Pap. **54**, 367–376 (2007)
23. J Miguez, L Castedo, in *Proceedings of the Ninth IEEE International Symposium on Personal, Indoor Mobile Radio Communications*, Boston. Blind multiuser interference cancellation in multicarrier CDMA: a linearly constrained constant modulus approach, vol. 2 (IEEE Piscataway, 8–11 September 1998), pp. 523–527
24. ML Honig, JS Goldstein, Adaptive reduced-rank interference suppression based on the multistage Wiener filter. IEEE Trans. Commun. **50**, 986–994 (2002)
25. RC de Lamare, M Haardt, R Sampaio-Neto, Blind adaptive constrained reduced-rank parameter estimation based on constant modulus design for CDMA interference suppression. IEEE Trans. Signal Process. **56**, 2470–2482 (2008)
26. DA Pados, GN Karystinos, An iterative algorithm for the computation of the MVDR filter. IEEE Trans. Sig. Proc. **49**, 290–300 (2001)
27. RC de Lamare, R Sampaio-Neto, Adaptive interference suppression for DS-CDMA systems based on interpolated FIR filters with adaptive interpolators in multipath channels. IEEE Trans. Vehicular Technol. **56**, 2457–2474 (2007)
28. RC de Lamare, R Sampaio-Neto, Adaptive reduced-rank processing based on joint and iterative interpolation, decimation, and filtering. IEEE Trans. Signal Process. **57**, 2503–2514 (2009)
29. RC de Lamare, R Sampaio-Neto, M Haardt, Blind adaptive constrained constant-modulus reduced-rank interference suppression algorithms based on interpolation and switched decimation. IEEE Trans. Signal Process. **59**, 681–695 (2011)
30. U Madhow, ML Honig, MMSE interference suppression for direct-sequence spread-spectrum CDMA. IEEE Trans. Commun. **42**, 1339–1343 (1994)
31. JD Chen, FB Ueng, JC Chang, H Su, Performance analyses of OFDM–CDMA receivers in multipath fading channels. IEEE Trans. Vehicular Technol. **58**, 4805–4818 (2009)
32. C Fugita, Y Hara, Y Kamio, Multiuser interference suppression in uplink multicarrier CDMA systems. IEICE Trans. Fundamentals. **E85-A**, 2256–226 (2002)
33. B Park, H Cheon, E Ko, C Kang, D Hong, A blind OFDM synchronization algorithm based on cyclic correlation. IEEE Signal Process. Lett. **11**, 83–85 (2004)
34. WL Chin, Chen S G, A blind synchronizer for OFDM systems based on SINR maximization in multipath fading channels. IEEE. T. Vehicular Technol. **58**, 625–635 (2009)
35. R Mo, YH Chew, TT Tjhung, CC Ko, A new blind joint timing and frequency offset estimator for OFDM systems over multipath fading channels. IEEE. T. Vehicular Technol. **57**, 2947–2957 (2008)
36. H Bolcskei, Blind estimation of symbol timing and carrier frequency offset in wireless OFDM systems. IEEE T. Commun. **49**, 988–999 (2001)
37. LJ Griffiths, CW Jim, An alternative approach to linearly constrained adaptive beamforming. IEEE Trans. Antennas Propagation. **30**, 27–34 (1982)
38. GH Golub, CFV Loan, *Matrix Computations*. (Johns Hopkins University Press, Baltimore, 1996)
39. X Dong, Z Ding, S Dasgupta, Performance analysis of a forward link channel estimation method for wireless multicarrier systems. IEEE Trans. Wireless Commun. **7**, 3026–3035 (2008)
40. D Darsena, G Gelli, L Paura, F Verde, Widely linear equalization and blind channel identification for interference-contaminated multicarrier systems. IEEE Trans. Signal Process. **53**, 1163–1177 (2005)
41. WA Gardner, Learning characteristics of stochastic-gradient-descent algorithms: a general study, analysis, and critique. Signal Process. **6**, 113–133 (1984)

doi:10.1186/1687-1499-2013-273
Cite this article as: Chen and Shen: **Adaptive constrained CM-based multicarrier-CDMA receivers in multipath fading channels.** *EURASIP Journal on Wireless Communications and Networking* 2013 **2013**:273.